March 2018

Design of a Compact Electromyograph Data Acquisition System

Alexander C. Rawley
Worcester Polytechnic Institute

Kevin Dian Lee
Worcester Polytechnic Institute

Xinyuan Zhang
Worcester Polytechnic Institute

Design of a Compact Electromyograph Data Acquisition System

Submitted to the Faculty of

Worcester Polytechnic Institute

in partial fulfillment of the requirements for the degree of
Bachelor of Science

Authors:

Kevin Lee

Xinyuan Zhang

Alex Rawley

Date:

February 8, 2018

Approved by:

Professor Edward A. Clancy

Abstract

Our team set out to design and prototype a compact electromyography (EMG) device that measures and records electrical signals associated with muscle activity. The EMG device was required to meet certain design requirements based on pre-existing designs, but improves upon certain key areas. The EMG device designed in this project begins at the electrode assembly, where input signals from the muscles are amplified by a fixed gain of 50 V/V with a common mode rejection ratio (CMRR) of over 100 dB at 60 Hz, a voltage noise level of less than 1 uVrms over the frequency range of interest (20-1800 Hz). The signal is required to be transmitted to a central signal processing electrical board. On the board, the signal enters a filtering stage with a passband of 15 Hz- 4 kHz before being digitized by a 24-bit sigma delta analog to digital converter (ADC). The ADC has a range of internal gain selections for each channel: 1, 2, 3, 4, 6, 8, and 12. The microcontroller is responsible for receiving, processing, and sending the digital signal, which is converted from the microcontroller's UART communication to serial USB format and sent to a computer through a USB communication cable. Using MATLAB, the signal data can be transferred into a computer platform to be used in other applications.

Acknowledgements

There are many people we can attribute the success of our project to including, but not limited to, Prof. John McNeill, Jianan Li, William Boyd, Prof. Stephen Bitar, Prof. Edward Clancy, and our team members. Prof. McNeill supported our understanding of Sigma Delta ADCs and brainstorming techniques. Jianan Li provided specific support about the ADC chosen for this project, as well as provided many hours of his time to help debug the system. William Boyd supported our team's understanding of MATLAB operations with background and foreground processes. Prof. Bitar helped identify several issues in our PCB design. Lastly, but surely not least, Prof. Clancy supported the group's understanding of EMG acquisition systems and helped develop the team throughout the twenty-one weeks of this project.

Executive Summary

Electromyography (EMG) is the procedure used to measure electrical activity in muscles. When signals travel from the brain down the spinal cord, and its associated nerve to a muscle fiber (commonly referred to as motor units), the electrical potential on the surface of the skin changes and can be measured. These signals range in magnitude from 100 uV to 10 mV depending on contraction strength and effort level, and have a frequency band of 20 Hz to at least 1000 Hz. An EMG acquisition device is used to quantify and record the electrical signals via metal electrodes. Two electrodes are placed a certain distance apart on the muscle of interest. There are two types of electrodes used to record this electrical potential in the muscle: needle electrodes and surface electrodes. Needle electrodes are long, thin metal conductors that are inserted into the muscle directly, while surface electrodes are placed on the surface of the patient's skin. The signal measured by the electrodes is amplified and filtered before becoming digitized by an analog-to-digital converter (ADC). The newly digitized signal can be further processed in software programs such as MATLAB or stored for further applications.

The project team was tasked with designing and prototyping an EMG acquisition device and electrode-amplifier that improves upon previous designs. The electrodes are expected to have a common mode rejection ratio of at least 100 dB at 60 Hz, with an input impedance greater than 100 MΩ, and a base gain of 50 V/V. The EMG acquisition device is required to be power and signal medically isolated to ensure the safety of the patient. There must also be a range of selectable gains including: 1, 2, 4, 8, 16, 32, 64, and 128 V/V, with an initial filtering stage gain of 5 V/V. The chosen ADC must operate fast enough to effectively sample the input frequency range (20 -1000 Hz) and be digitized in at least 24 bits. Overall, the system must consume less

than 500mA of current in order to be powered by USB and should be lightweight enough to fit on a person during normal operation.

To meet the design specifications, the project team designed three PCBs: One for the electrode-amplifier, one for the main signal processing board, and one for peripheral connections. The electrode-amplifier PCB contains an instrumentation amplifier with a 1 kΩ gain setting resistor and a 15 uF capacitor with a cutoff at 10 Hz. The instrumentation amplifier has a base gain of 50 V/V and an input impedance above 100 MΩ. The electrode amplifier was encased in a 3D-printed shell filled with resin and wired via a four-conductor shielded cable connected to a micro USB B male connector. Each peripheral PCB contains 8 micro USB B female connectors that wire to male jumper pins for connecting to the main signal processing PCB. The main signal processing PCB can connect to two peripheral boards, or 16 electrode channels, at once. Input signals from the electrode-amplifiers pass through a second order Sallen-Key high pass filter with cutoff at 15 Hz and an RC low pass filter with cutoff at 4 kHz. Overall this filtering stage amplifies the input signal by 5 V/V. Output signals from the filtering stage enter one of two ADS1298 ADCs, which can sample each channel at 0.5, 1, 2, 4, 8, 16, and 32 kSPS and has an integrated individual channel gain of 1, 2, 3, 4, 6, 8, and 12 V/V. Data processing and transfer to a PC is handled by a microcontroller with a 32 MHz base clock. Processed data are sent over UART communication at 128,000 bps to a "UART to Serial" converter chip, through the signal isolation chip, and to the PC where further processing can take place for various applications. The PCB has both power and signal isolating surface mounted chips. The power isolator can source up to 400 mA of current at 5 V which can safely be provided by the USB 2.0 port of a PC, removing the reliance on external power supplies.

Figure 1 details the overall system topology of the hardware. Figure 2 shows the prototype signal processing board and peripheral connection boards. Figure 3 shows the final electrode amplifier design.

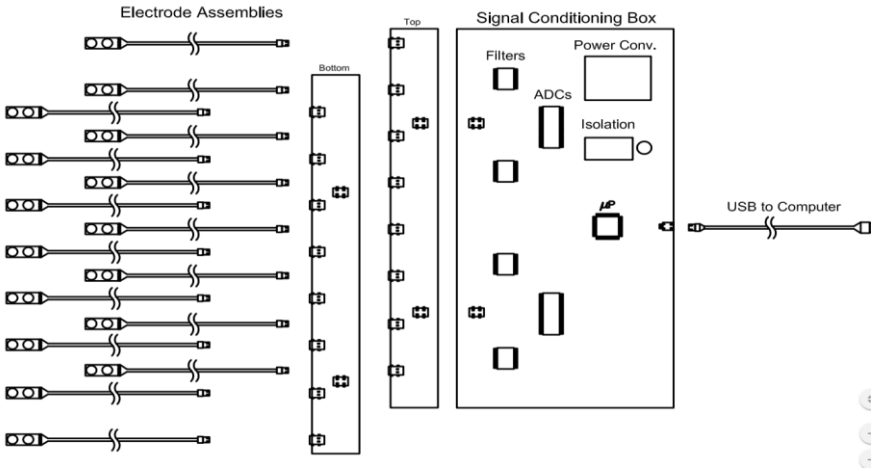

Figure 1: Final System Topology

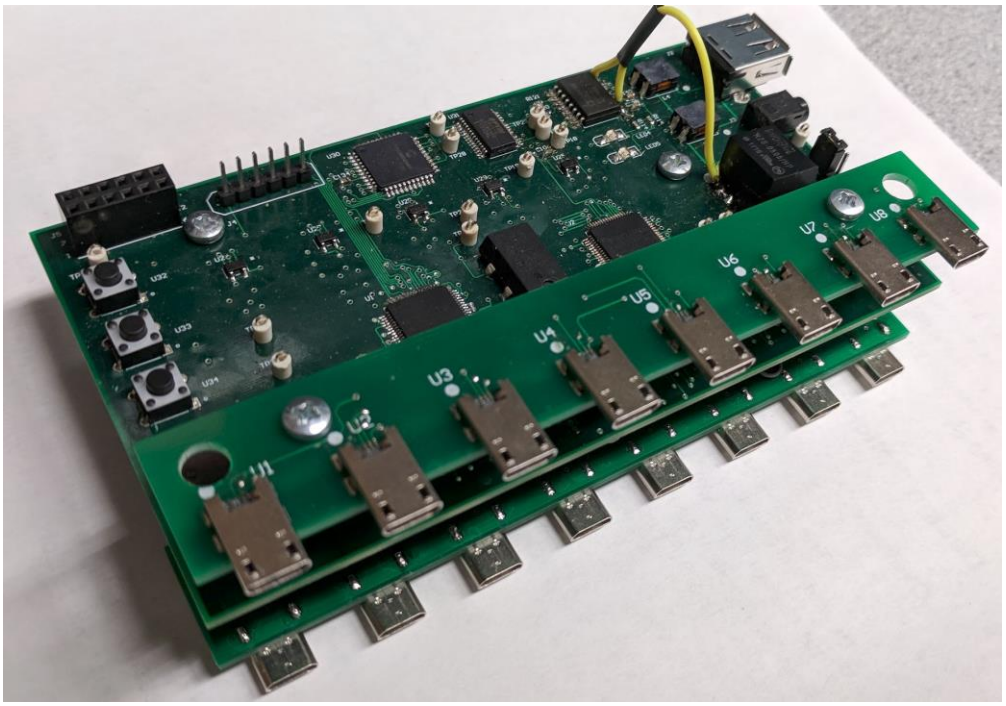

Figure 2: Signal Processing and Peripheral PCBs

Figure 3: Electrode Amplifier Encasement

Besides hardware, software is also necessary to make the project device function properly. There are mainly two programs designed: one for the microcontroller, another for MATLAB. The main task of the program in the microcontroller is to communicate with two ADS1298s, pulling data from these ADCs, and transmitting data to the computer. To complete these tasks, the microcontroller program consists of several modules: system configuration, timer, SPI, UART, ADS1298 modules, and the main function. The microcontroller program also has a command system that accepts commands from the computer (via MATLAB) and applies corresponding settings. The MATLAB script interacts with users, accepts data from the microcontrollers, and converts the data from ADC count to voltage. The sample data are stored in MATLAB for further processing if it is necessary.

During normal operation, the electrodes should be appropriately placed on the human body along with a reference electrode that connect the device's power ground (the reference for the ADC) to the human body.

Due to the limitation on microcontroller operating speed, the prototype project device can only operate with one eight-channel ADC at a maximum sampling rate of 1 kSPS, with a 3 dB passband from 0 to 260 Hz. This speed limitation also prevents implementation of many other functionalities, such as software gains in the microcontroller, and lower, variable data rates. The speed issue could be solved by using a faster signal processing unit. Doing so was beyond the scope of this work. There are also other improvements could be made in the future. The ADS1298 uses a digital filter with a narrow pass band, which results in limited input bandwidth. To solve the narrow pass band issue, an extra filter could be implemented to extend the pass band, or faster ADCs rates could be used. Using smaller electronic component packages could make the electrode design even smaller. Smaller electronic components and more powerful Ics could also make a more compact design possible. Everything up until the signal processing unit could be put on the electrode circuit boards if small and powerful electronic components were available.

One of the major portions of this project was the electrode amplifiers. These amplifiers had a noise level of 0.693 uVrms RTI, a high pass cutoff of 13 Hz, a gain of 50 V/V, a CMRR of 103 dB at 70 Hz, and a small package size of 3.18 cm x 1.19 cm x 0.51 cm. The main PCB board is roughly 3 in x 5 in x 4 in. The main board has a current draw of less than 300 mA, and an overall system noise of 0.694 uVrss RTI. The ADC offset is 0.0178 V at the input of the ADC. Lastly, the 2^{nd} order Sallen-Key high pass filter has a cutoff frequency of 15 Hz with a low pass anti-aliasing filter cutoff of 4 kHz.

Table of Contents

Table of Figures

Table of Tables

1 Background

1.1 Introduction

Electromyography, commonly known as EMG, is a procedure used to measure electrical signals from muscles throughout the body. Electrical activity of the muscles is recorded through electrodes placed on or in the body and is used to monitor the physiologic function of muscle, including possible muscle dysfunction or disease. The goal of this project was to investigate different methods and approaches to designing a surface EMG acquisition system and successfully implement a working system.

1.1.1 Synaptic Transmission and Motor Unit Action Potentials

Synaptic transmission is the process of sending signals from the spinal cord to other nerves and muscle fibers (Lerner, 2014). The central nervous system (CNS) sends signals in the form of chemically induced electrical potentials that travel the length of the nerve. Figure 4 below shows the spinal cord nerves and how they connect to muscle fibers throughout the body.

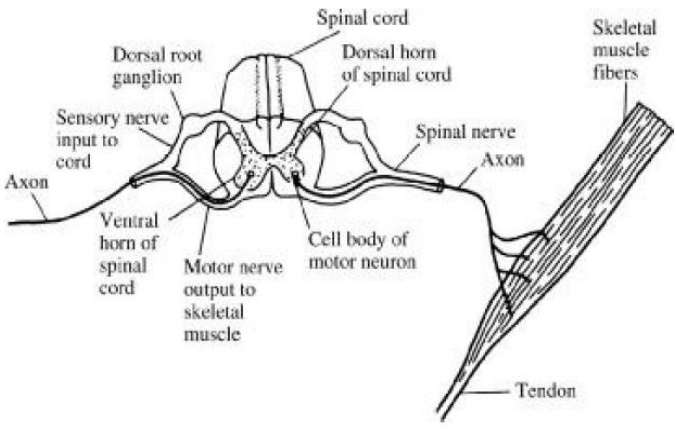

Figure 4: Illustration of Spinal Nerves Connecting to Muscle Fibers (Webster, 2010)

A nerve membrane is typically polarized, with the inside of the membrane more negative than the outside of the membrane at a resting voltage of around -70 mV. As a nerve cell receives a transmission signal from the CNS or another neuron, channels in the cell membrane open and depolarize the membrane, causing the inside of the membrane to become more positive until the electrical potential reaches a biological threshold voltage. Passing this threshold voltage will cause the adjacent membrane channels to open progressively along the length of the axon and propagate the signal down the length of the neuron (Burt, 2016). These signals, called action potentials, can travel across neurons before reaching the destination motor unit. When the signal reaches the motor unit, the electrical potential triggers muscle contraction in the surrounding area. Some motor units can be acted upon by more than one nerve which decreases the amount of time between action potential firings (Slater, 2015). Varying levels of contraction strength can be achieved by varying the number of active motor units and the rate at which the motor units are activated. Muscle stimulation signals, which dictate the activation rate of motor units, can range in frequency between 4 and 20 Hz (Slater, 2015). An EMG is able to record electrical activity of muscles due to biological interaction.

These electrical potentials moving across multiple muscle fibers create extracellular field potentials that can be detected and used to measure electrical activity in muscles (Merletti and Farina, 2016). EMG devices are used to measure the electrical signal through electrodes, which detect this extracellular field potential in the form of a voltage potential.

1.1.2 Characteristics of Electromyography Signals

With the advance of technology, the development of EMG acquisition systems have bridged the gap of human understanding of skeletal muscle activity. EMG is a method of recording and quantifying the electrical activity produced by depolarization and repolarization of the outer muscle fiber membrane, which is related to motor unit activities (Lee, 1996). During muscle contraction, the electrical potentials induce electric fields that can be detected through electrodes, as shown in Figure 5. Thus, the potential generated by a motor unit can be measured (Merletti and Farina, 2016).

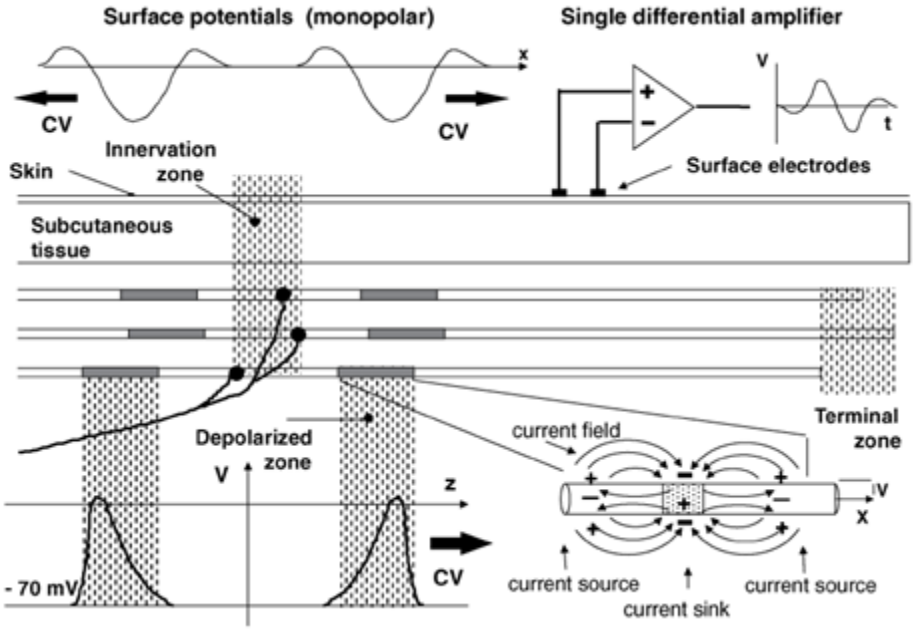

Figure 5: EMG Signal Induction (Merletti and Farina, 2016)

Similar to other human biological signals, the measurement of EMG signals is a constant battle with interferences. The raw surface EMG signal has an amplitude range of approximately 0-10 mV peak to peak. It has a primary energy in the frequency range of approximately 0-500 Hz as shown in Figure 6. The dominant frequency range is 50-150 Hz (Gargiulo, 2011). With

increased muscle effort, the signal may be above the noise floor at frequencies of up to 1800 Hz. The signals are so small that any substantial interferences and electrical noise can affect EMG measurement. The most common sources of interference include the following:

(1) Motion artifacts caused by variation, or momentary loss of electrode-skin contact.

(2) Movement of cables connected to the electrodes.

(3) Power-line interference coupling.

(4) Change of noise levels due to contact quality fluctuations.

(5) Electrode-skin interface noise.

The measured EMG signals also have a DC offset voltage caused by static half potential interference (Merletti and Farina, 2016; Webster 2010).

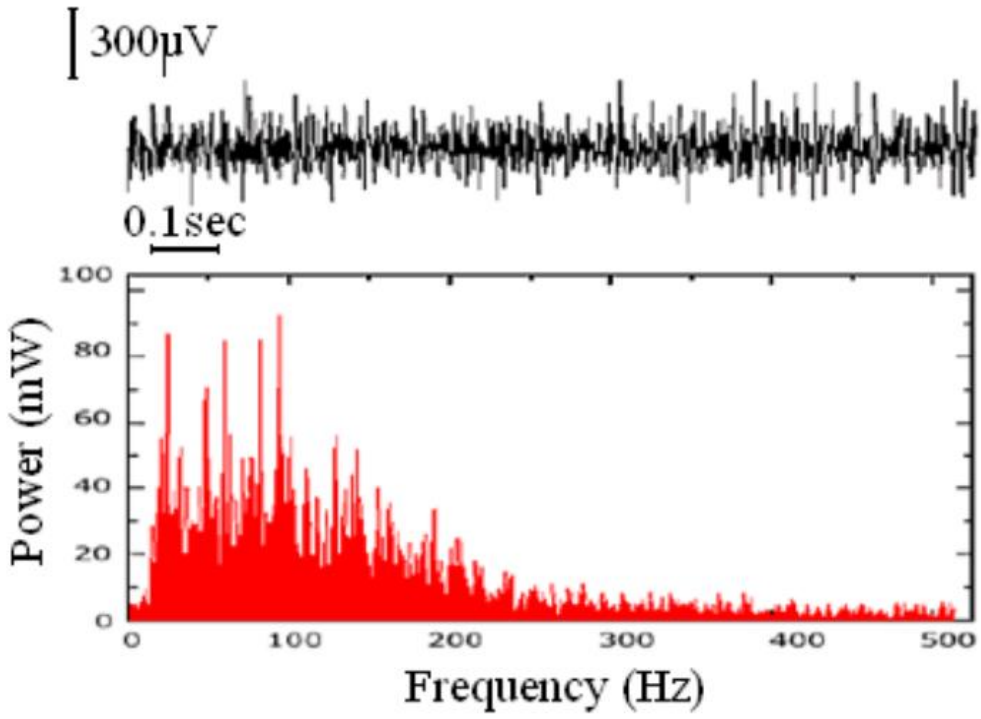

Figure 6: A Noisy Signal (black) and Power Spectrum (red) (Gargiulo 2011)

1.2 Types of EMGs

There are two main methods in recording EMG signals, invasive and surface acquisition. The first method uses a wire or needle inserted into the muscle directly. The second method uses surface electrodes, such as metal studs, which are placed and secured to the surface of the skin. Needle EMG and surface EMG are used for completely different purposes and have their own advantages and disadvantages, explained in further detail below.

1.2.1 Surface EMGs

Surface recordings of ongoing background EMG are more suitable for long-term recordings and are not selective, meaning that they can pick up signals from many motor units at any given time, depending on the distance between electrodes. An increase in the amount of motor units may result in signal crosstalk, which happens when the surface EMG signal from one muscle interferes with that of another. Specific techniques can be used to minimize crosstalk between these signals. Surface recordings are used in many applications such as prosthetic controllers or as a control signal for computers and other devices (Burke, 2010). Surface EMG signals consist of two electrodes that contact the skin with a third electrode used for reference voltage. Figure 7 shows an example of a raw surface EMG signal during isometric contraction. The individual motor unit potentials are not visible, since the surface EMG picks up signals from many different motor units at the same time.

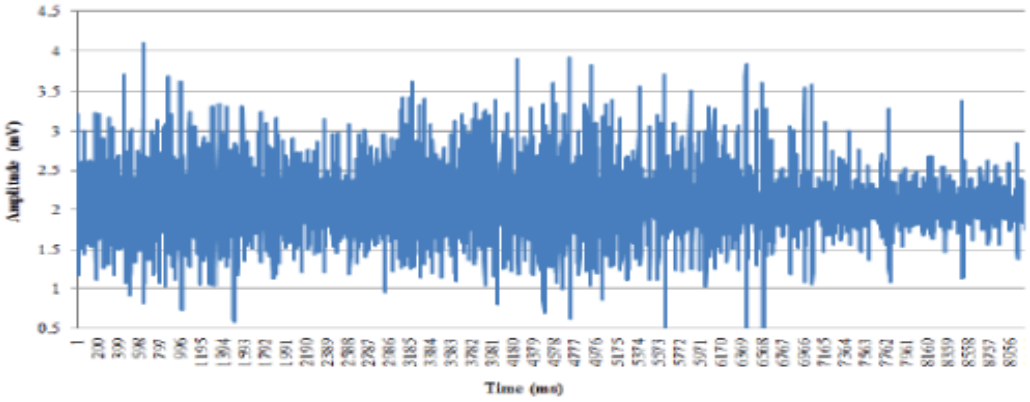

Figure 7: Surface EMG Signal During Isometric Contraction (Ahamed et al. 2016)

A disadvantage of using the surface EMG technique is that the surface electrodes can only be used with superficial muscle groups (muscles close to the surface of the skin) and are prone to irregular measurements due to electrical activity over a wide area (Webster and Clark, 2010). Electrode pairs are attached with the electrodes oriented in parallel with the length of the muscle fiber in order to best record the total electrical potential fields generated by the action potentials transmitting across them. The signals detected are the total of multiple motor unit action potentials (MUAP) detected at various distances from the action potential source. These MUAP signals can be distorted by the spatial low pass filtering effect of the tissue separating the sources and the recording electrodes. The MUAP from one motor unit can combine with the MUAPs of other motor units. For this reason, there are invasive means to detect action potentials of a small number of muscle fibers. (Merletti and Farina, 2016)

1.2.2 Needle EMGs

Needle EMG studies have been performed as far back as 1929 which originated as observational tests in cats by Adrian and Bronk who used a concentric needle electrode, similar to what is commonly used today (Burke, 2010). Figure 8 below shows commonly used types of needle electrodes.

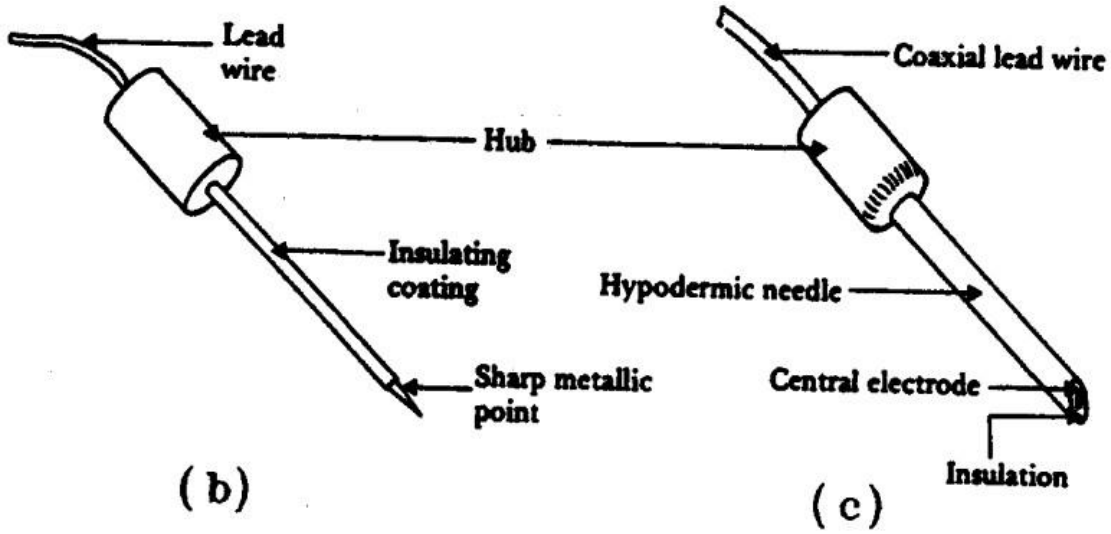

Figure 8: Needle Electrodes (Neuman)

Needle electrodes are inserted into the muscle at a set location. Techniques range from using specialized electrodes to study a single motor unit, such as single fiber EMGs, to combined recording of an entire motor system. In standard needle EMG practice, needle electrodes are inserted into the muscle of interest. Each needle contains insulated wire with a standard recording area of 125x580 um. By inserting the electrode directly into the muscle fibers, it is easy to accurately measure electrical characteristics of the motor unit (Thornton, 2012). Figure 9 shows an example of the measurements from needle EMG. At low level muscle contraction, single motor unit potentials can be measured by the needle EMG as shown in Figure 9(a). As muscle contraction level increases, the single motor unit potential is no longer recognizable in the measurements.

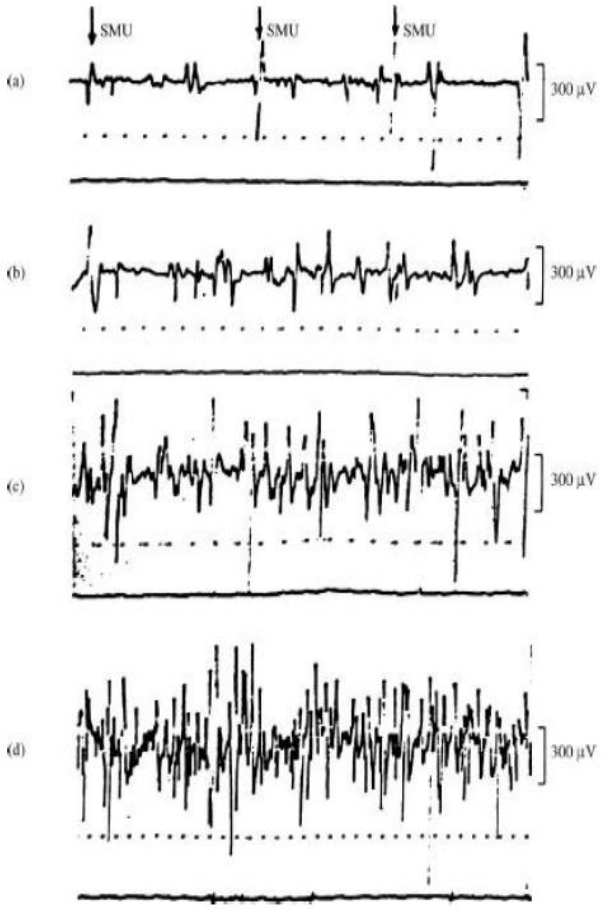

Figure 9: Needle EMG Measurement During Progressive Contractions (Webster 2010)

Although needle EMGs have excellent sensitivity, they are limited by spatial undersampling. Inserted electrodes record primarily from motor units lying 1-2 mm around the electrode tip (Thornton, 2012). Only a small number of motor units can be sampled at a given time, which is not ideal for larger muscle recordings. Needle EMGs are also not ideal for long term use due to the invasive nature of indwelling electrodes, which can cause discomfort to the patient.

1.3 Functions of EMG signals

By studying EMG signals, researchers and doctors gain deeper understanding about muscle activity and human motion control, which inspire applications on certain disease detections and prosthetics. The shape of single motor unit potentials can be modified by disease. In peripheral neuropathies, partial denervation of the muscle frequently occurs and is followed by regeneration. Regenerating nerve fibers transmit action potentials slower than healthy axons. In many forms of peripheral neuropathy, the excitability of the neurons is changed and there is widespread slowing of nerve conduction in the repaired axon (Webster, 2010). By looking for abnormal EMG signals, doctors have higher chances to identify the causes of peripheral neuropathy, and prescribe appropriate treatments.

EMGs are also used in non-medical applications; myoelectrically controlled upper-limb prosthetics have been a driving force in EMG development. EMG signals from remnant muscles have been used to control the operation of a prosthetic elbow, wrist, and/or hand. For patients with an amputated upper arm and forearm, the electrical activity of two muscle sites is monitored primarily in the biceps and triceps muscles. A common methodology is to estimate the EMG standard deviation from the two sites, and use these signals to determine the corresponding actions of the prostheses. To determine the standard deviation of the EMG signal, two parameters are commonly calculated. The first parameter is the average value of the rectified EMG signal, referred to as the Average Rectified Value (ARV) or the Mean Absolute Value (MAV). The ARV corresponds to the mean value of the absolute amplitude over a given period of time or to the low pass filtered rectified value. The other parameter is the root mean square (RMS) value, whose square represents the variance, which is the power of the signal. Although

the association between EMG and force is not always linear, the standard deviation of EMG is still an appropriate measure of muscle activity. (Merletti and Farina, 2016)

1.4 Stages of EMG Acquisition Systems

The first main component in a system to capture electromyographic data is a pair of electrodes. The electrodes carry out a transducing function, because in the body current is carried by ions, whereas in the electrode-amplifier and its lead wire, current is carried by electrons. Electrodes serve as transducers to change an ionic current into an electric current that can be recorded. Typically, researchers have used stainless steel, platinum, or gold-plated electrodes to minimize the chance of material contamination interfering with chemical reactions with perspiration or gel (Webster, 2010). After the signal is transduced on the electrodes, the signal propagates through a differential amplifier which provides a signal which can be analyzed and processed by a computer or other software. The differential amplifier takes the difference between its two inputs and amplifies this new signal to a voltage that can be more readily observed and transmitted down wires without inheriting additional noise. The difference between the signals at the two electrodes represents the change in voltage as a result of the electrical impulse moving down the muscle fiber. Surface mounted electrodes exhibit intrinsically noisy and widely variable impedance depending on the electrode metal and size as well as the gel and skin condition of the patient. The variance in skin impedance affects the noise and signal integrity of the surface electrodes. When an input current bias for an amplifier is constant, there will be an input current noise (voltage) that is proportional to the skin impedance. Filters are often used in order to reduce the effect of noise on the signal of interest by cutting off frequency bandwidths of known noise sources.

Another common problem that electromyographers face is parasitic capacitances with the power line and ground as these form voltage dividers and can potentially generate interference voltages in a larger magnitude than the EMG signal being recorded on the skin. The detection system must reject this interference as much as possible in order to reduce the risk of saturating the amplifier circuit (Merletti and Farina, 2016). An isolation stage is often involved in the signal chain as a safety precaution. Isolation amplifiers break the signal path between the input and output and prevents leakage currents from flowing to the patient through the electrodes. The three main types of isolation are transformer isolation, optical isolation, and capacitive isolation. The transformer isolator uses a frequency-modulated or a pulse-width-modulated carrier with signal bandwidths up to 30 kHz to carry the signals. The optical approach uses a LED on the source side and a photodiode on the output side. Lastly, the capacitive approach uses digital encoding of the input voltage and frequency modulation to send the signal across a differential capacitive barrier (Webster, 2010). The isolation stage is key for patient safety and is required in all medical grade equipment.

As the signal will be recorded and possibly displayed using a computer, an analog-to-digital converter (ADC) is used to digitize the signal, after which a microprocessor (uP) is used to communicate with a port on the computer. ADCs use bit resolution to take the analog signals from the patient and output a corresponding discrete value that can be used by a computer or digital software. The conversion process involves quantizing and encoding. Quantizing means separating the analog signal range into a number of discrete quantities and determining which analog signal level corresponds with which discrete digital value. Encoding means assigning a unique digital code to each analog level and determining the code that corresponds to the input signal. Increasing the number of bits used in the conversion process provides more quantization

levels to divide the input signal into, and thus records the signal at a finer resolution. (Sheingold, 2014)

1.5 Previous Surface EMG Acquisition System Designs at WPI

A number of existing EMG acquisition systems have been built by different project teams at WPI for lab and research usage in the past. The hardware and software designs for each system are different due to available parts and technology at that period of time. The first system, designed by Professor Ted Clancy, was built in 2005. A second system, built in 2015, is a simplified version of the first with a more compact design. It is important to review the existing systems before describing the system designs for this project. (Clancy, 2002)

1.5.1 Surface EMG acquisition system from 2005

In 2005, a group of Electrical and Computer Engineering students at Worcester Polytechnic Institute designed and built a wired 16-channel system for acquiring the surface EMG signal from the human body, under the guidance of their advisor Professor Ted Clancy. The system consists of front end electrodes, signal conditioning stations, and power supplies. Figure 10 provides an overview of the system. The eight white boxes are the signal conditioning stations. Each of which contains four channels. They have manual dials for selecting gains. The two boxes to the right in Figure 10 are power supplies, one medically-isolated, and the other earth-grounded. There are sixteen front end electrode-amplifiers connecting to the signal conditioning stations with wires, not all of which are used in this system. (Clancy, 2002)

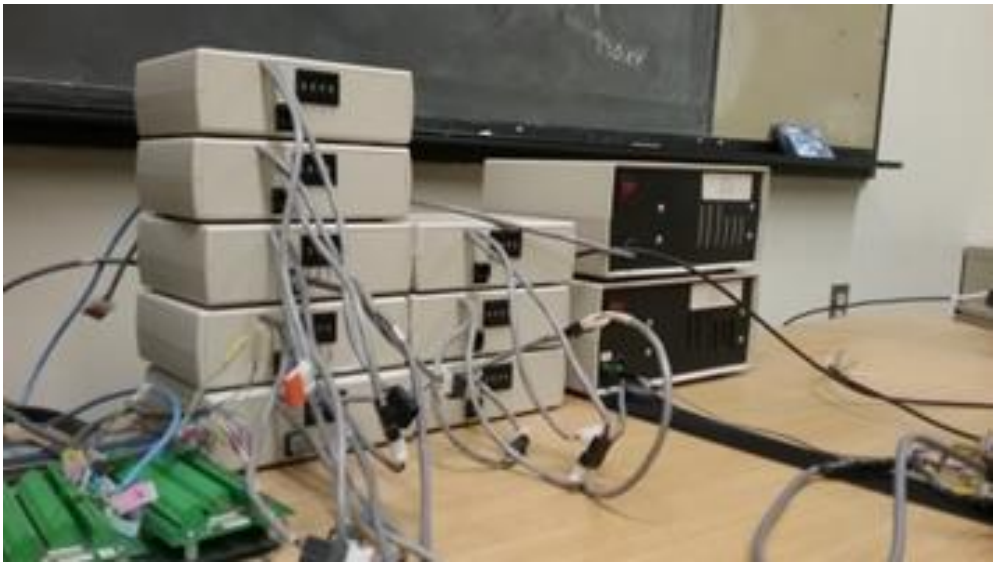

Figure 10: The EMG Acquisition System from 2005 (Clancy, 2002)

An encased front-end electrode-amplifier was designed with an instrumentation amplifier and two stainless steel screws as contacting electrodes. Figure 11 shows a typical instrumentation amplifier model. The impedance Z_G decides the gain of the instrumentation amplifier. Typically, the impedance Z_G is implemented with a resistor. However, by inserting a capacitor in series with the resistor, the instrumentation amplifier will exhibit a high pass characteristic, which is desired for attenuating low frequency noise, such as motion artifact, and DC offset signals. For the 2005 system, the instrumentation amplifier AD620 (Analog Devices) was used with a simple resistor used to set the gain (no high pass filter effect). This system provides an input impedance exceeding 100M Ω, a low output impedance, noise below 1 uV referred-to-input (RTI), a common-mode rejection ratio greater than 100 dB at 50/60 Hz. The instrumentation amplifier gain was set to twenty, but it was noted that a higher front end gain would be more desirable. A small PCB was designed to house the active front end electrode. The two screws used as contact electrodes were locked to the PCB with two nuts. These nuts also serve as electrical contact points between the PCB traces and the screws. For the electrode housing, the 2005 system used

epoxy to encapsulate the PCB as shown in Figure 12. Flexible Cooner brand wires were used as the connection between the front end electrodes and the signal conditioning stations (Clancy, 2005).

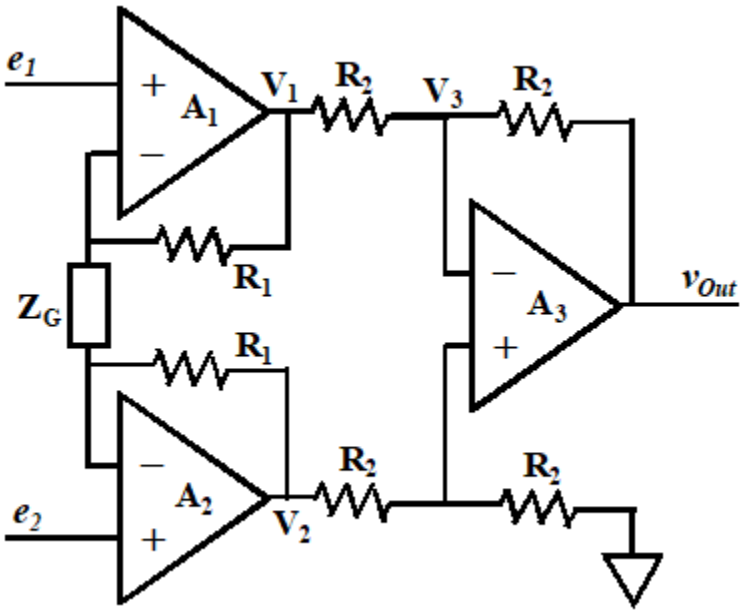

Figure 11: A Typical Instrumentation Amplifier Model (Clancy, 2005)

Figure 12: The Front End Electrode for the System from 2005 (Clancy, 2005)

In the electrode shown in Figure 12, the inter-electrode distance is 1 cm (edge to edge) and the case measures 3.8 cm tall by 1.6 cm wide by 1.1 cm thick. Figure 13 shows the signal conditioning circuit design for one channel. The front-end electrode connects to the circuit to provide the input signal V_{In}. A 100 kΩ pull down resistor at the very front prevents floating signals at unused channels which could be misinterpreted as usable data. The first stage after the

electrode-amplifier is an eighth-order Sallen-Key high pass filter with a cutoff frequency of 15 Hz and a gain of 10 V/V. This high pass filter stage can provide a sharp cutoff before the 3 dB point to further attenuate the low frequency noise. This filter also provides extra gain to the system. Following the high pass filter stage is a selectable gain circuit implemented with a non-inverting amplifier circuit and analog switches. By changing the value of the resistor that connects the negative terminal of the op-amp to ground, the circuit can provide eight selectable gains of 1, 2, 4, 8, 16, 32, 64, 128 V/V. The total system gain ranges from 200 to 25,600 V/V. These gain options can be used to accommodate a large range input signal. There is a simple passive high pass filter circuit after the selectable gain stage to remove any offset voltage added by the operational amplifier in the gain stage. Following the selectable gain stage is a signal path electrical isolation circuit. This system uses a precision linear optical isolator to protect system users from potential leakage currents due to component or circuit faults. Besides the signal path isolation, the power supply is also isolated to meet the medical isolation standard. The last part of the circuit is a fourth-order Sallen-Key low pass filter stage with a cutoff frequency of 1800 Hz and a gain of one. This filter stage is used right before the signal entering the ADC to prevent signal aliasing. A passive high pass filter is also implemented after this stage to remove any offset voltage added by the operational amplifiers. After the input signals go through the signal conditioning stations, they are fed through a buffer into a 16-bit ±5 V ADC on a PC to turn into digital signals for further signal processing. (Clancy, 2002)

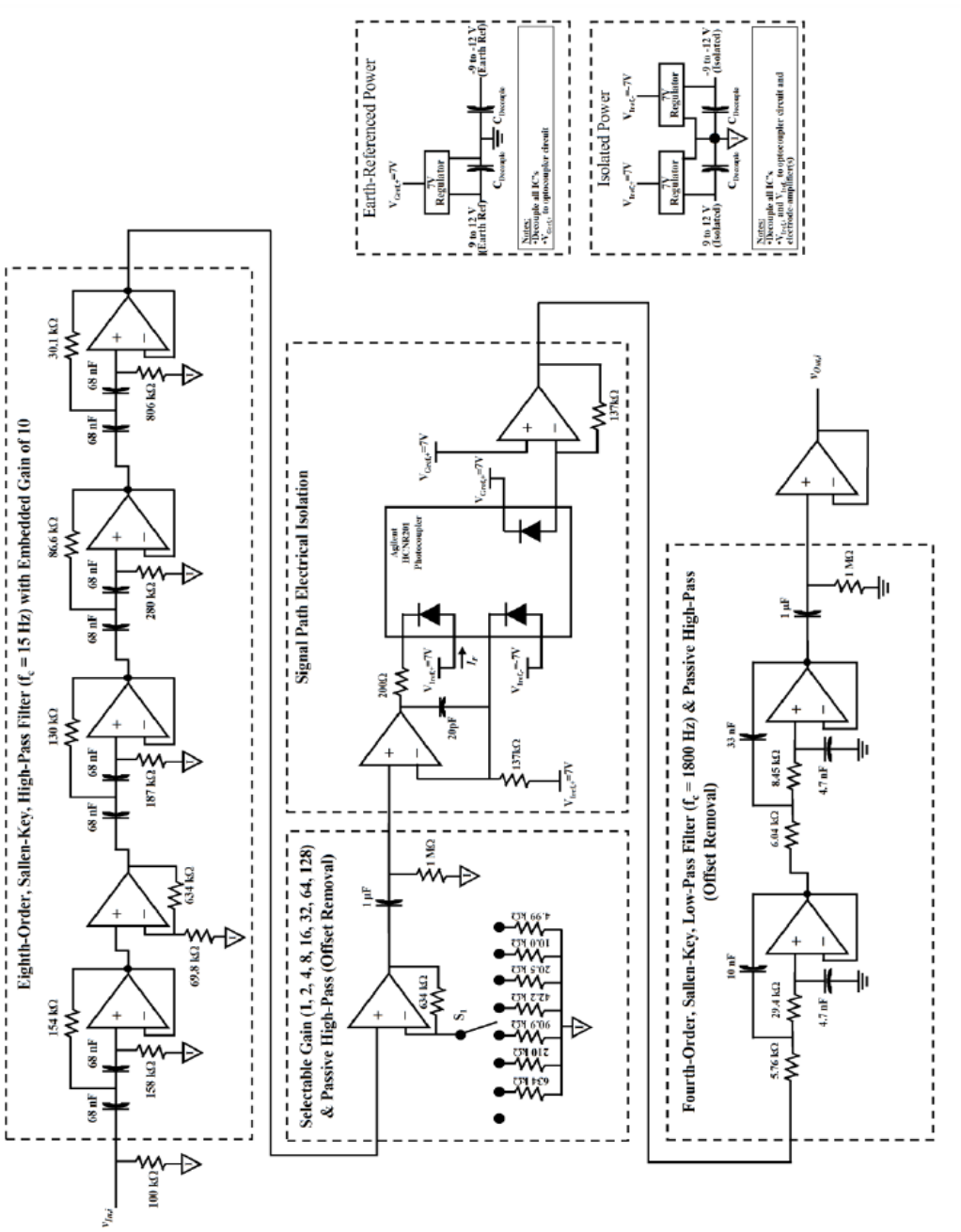

Figure 13: EMG Acquisition System from 2005 Without Front End and ADC (Clancy, 2005)

1.5.2 Surface EMG acquisition system from 2015

After ten years, a more compact system was built by Professor Clancy. The system is called the EMG-Force Acquisition System. It is a laboratory system to acquire sixteen bipolar EMG recordings from able-bodied patients as well as limb-loss subjects. This system also records the outputs of a six-axis force transducer. The force transducer system is not related to the topic of this report, therefore it is not discussed here. Figure 14 shows the overview of the EMG Acquisition System. The system was built around a PC with on-board 32-channel, 16-bit, 2.8 MS/s ADC. The general concept of the system is similar to the system from 2005, except there are some improvements and differences between the two designs. (Clancy, 2015)

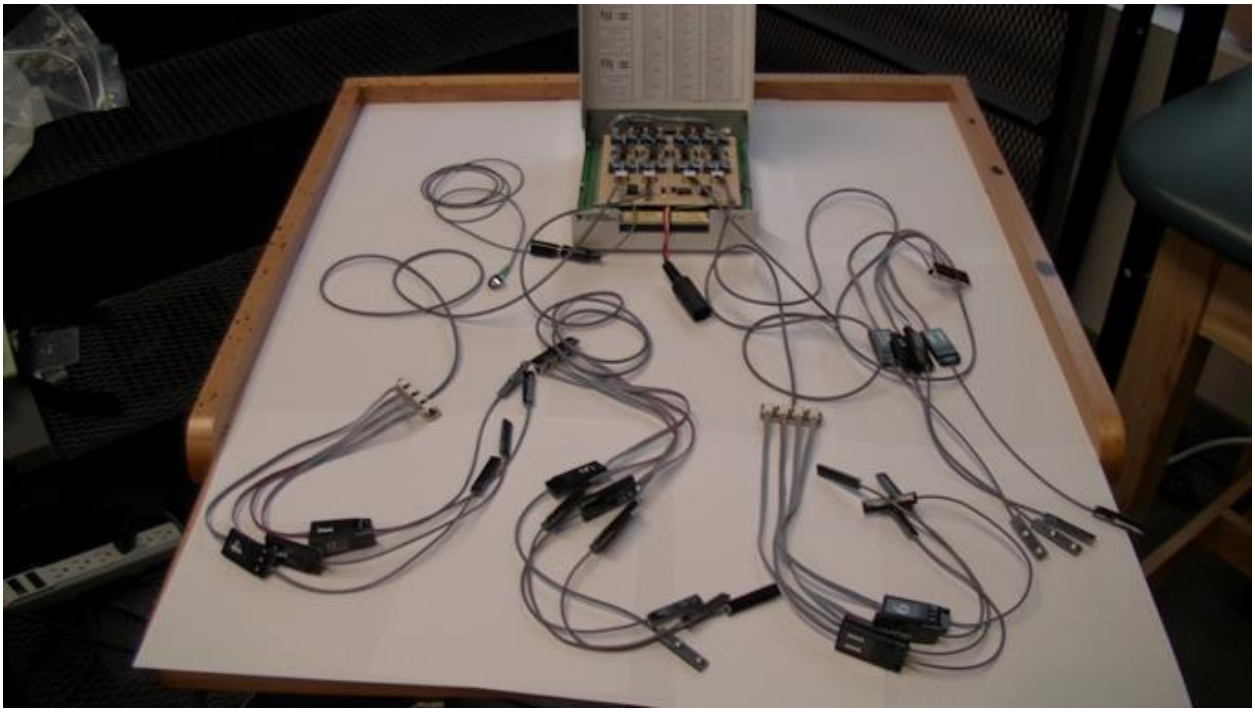

Figure 14: The Overview of the EMG Acquisition System from 2015 (Clancy, 2015)

In the 2015 system, the front end electrodes were designed differently. A pair of 0.5 cm diameter Liberating Technologies Inc. (LTI) dome electrodes were held in a fixed position with a plastic tab and was designed with a 3D printer and CAD modelling software. The electrode pair is wired directly to an LTI brand amplifier that has a passband from 30-500 Hz, a CMRR greater than 100 dB at 50/60 Hz, and a gain of 850 V/V. Since the amplifier is not built into the front end electrode, the encased electrode is much smaller compared to the one from 2005. Conversely, since the first-stage front end electronics are placed further away from the electrode contacts, this system may be more susceptible to noise. A group of four of these electrode sets (shown in Figure 15) is connected to the EMG gain electronics, which is implemented inside a 68-pin Shielded Desktop Connector Block. (Clancy, 2015)

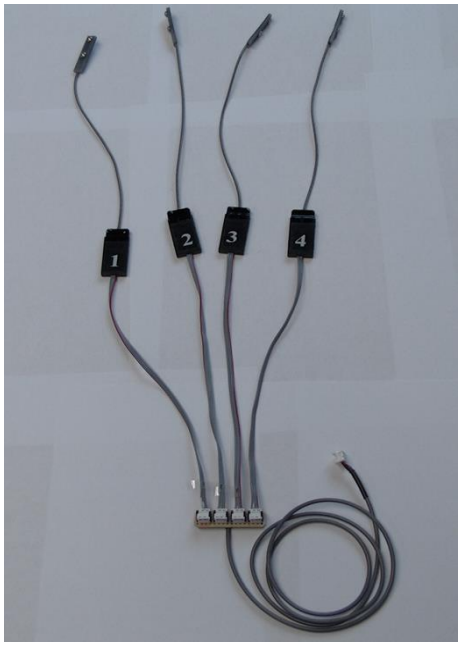

Figure 15: A Connector Block, With Four Front End Electrode Sets (Clancy, 2015).

The primary purpose of the gain electronics was to provide selectable gain to each signal. A general circuit diagram for one EMG channel is shown in Figure 16. These gain electronics

include a non-inverting amplifier circuit with switching resistors. The input is the signal from the electrode-amplifier and the output is connected to the ADC. Through a six-position switch, users can change the gain of the channel by switching between different resistors. The available gains are 1, 2, 4, 8, 16, 32, and 64 V/V. With the selectable gains, the system has a total gain range from 850 to 54,400 V/V. The input and output of the amplifier circuit are each connected through a passive high pass filter. These high pass filters have a gain of 1 and a cutoff frequency of approximately 0.16 Hz. They are used to remove any DC offset voltage from the electrode amplifier and the selectable gain amplifier. (Clancy, 2015)

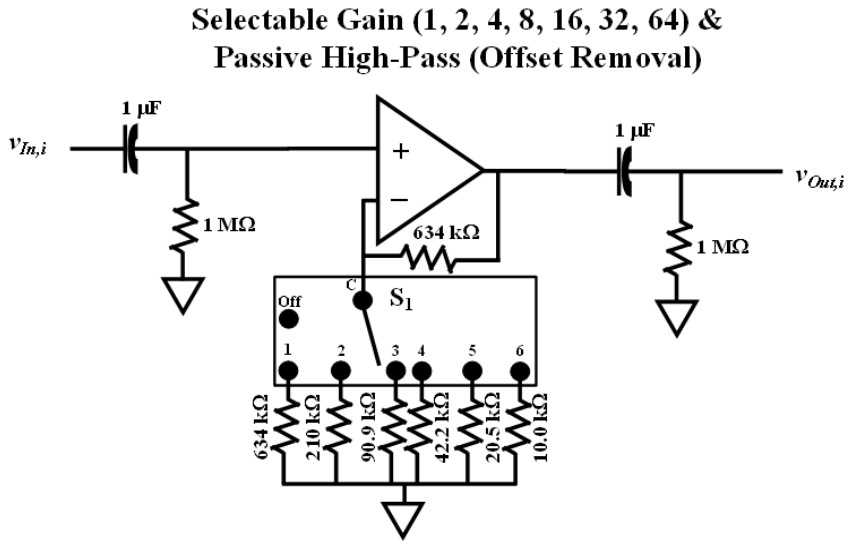

Figure 16: General Circuit Diagram for One EMG Gain Channel (Clancy, 2015)

This system is isolated from earth ground to protect users from any electrical damage. The entire PC and the load cell are powered by a medical grade AC power isolation transformer. Due to the fact that the whole system is connected to the ADC within the PC, the system is also isolated. (Clancy, 2015).

2 Project Design Specifications

The design chosen to perform EMG signal acquisition in this project has specific requirements chosen to produce a high quality laboratory-use system. These requirements include accepting an input signal with voltage range from 100 uV to 10 mV. The lowest signal was chosen to be 100 uV as certain patients with missing limbs can have an EMG level much smaller than regular patients. The system will be able to accommodate signals up to 1000 Hz as previous laboratory research has shown the energy density spectrum increasing in amplitude with effort level, leading to the signal being above the noise floor at higher frequencies. To reject the interference from the power line, the Common Mode Rejection Ratio (CMRR) will be greater than 100 dB at 60 Hz. In order to directly measure the voltage on the skin, the input impedance of the device must be greater than 100 MΩ in order to be 100 times the maximum skin impedance. A high impedance is required due to a voltage divider effect that forms between the skin impedance and input impedance of the instrumentation amplifier. The instrumentation amplifier in combination with the Sallen Key high pass filtering will apply a base gain of 250 to the input signal before the selectable gain stage. In order to accommodate a large range of input voltages, the system must have selectable gain levels of 1, 2, 4, 8, 16, 32, 64, and 128 (with 250 V/V base gain). This selectable gain will be used to fill up the dynamic range of a 24-bit ADC to provide a high precision recording of the analog input voltage on the skin. The system must be medically isolated electrically in order to protect the patient from electrical shock. Finally, the current consumption of the system must be low enough to be powered off of a single USB 2.0 port. The current output of the USB 2.0 ports is typically 500mA, however, after power isolation the total current available is roughly 300mA. These design options, among others, are outlined in Table 1 below.

Table 1: Design Specifications

Design Specifications	
Input Signal Amplitude	100 uV to 10 mV
Input Signal Frequency	20 to 1000 Hz
CMRR	Greater than 100 dB at 60 Hz
Input Impedance	Greater than 100 MΩ
Selectable Gain Levels	(1, 2, 4, 8, 16, 32, 64, 128) x 250 (Base gain)
ADC	At least 24 bit
Isolation	Medically Isolated
Current Consumption	Less than 300 mA
Size/Weight	Ideally small/lightweight enough to fit on a person as data is being recorded

3 General Design Topography

From the design specifications, the general design topography of the system is generated. Figure 17 below shows the general topography of the EMG acquisition system design.

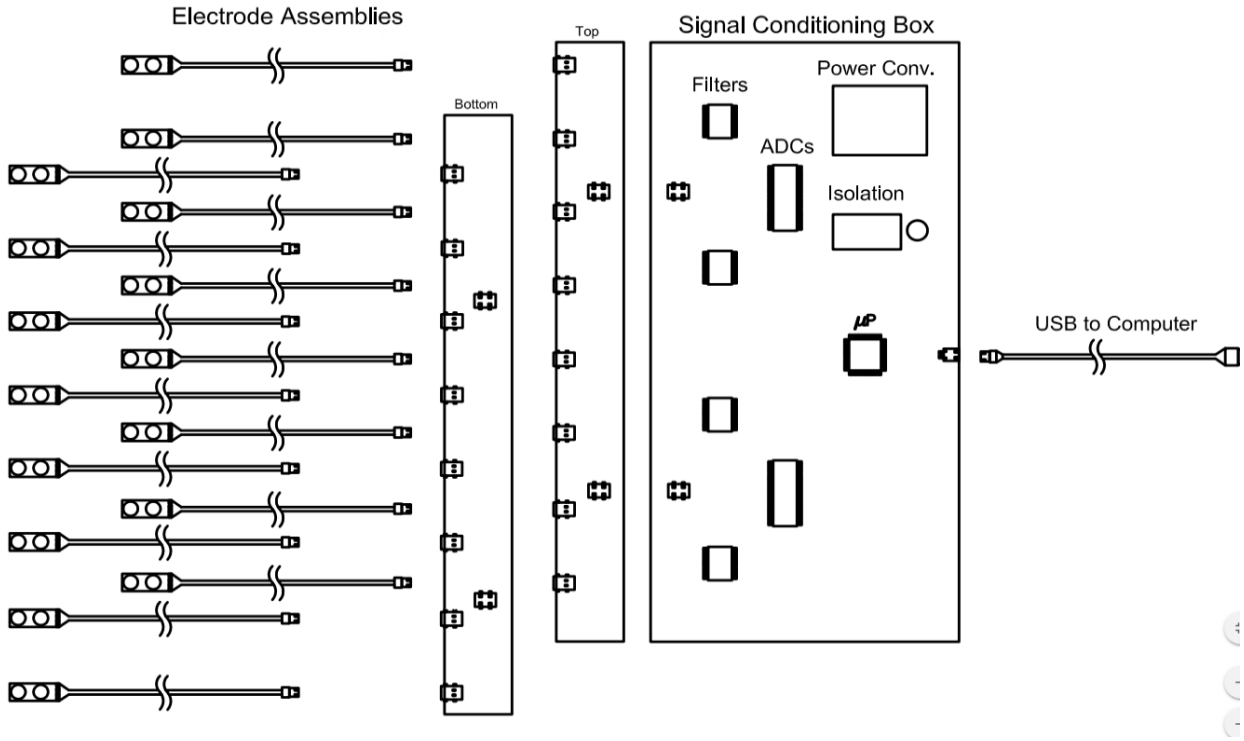

Figure 17: Generalized EMG Topology

Each of the 16 front-end electrode-amplifiers connect to the “Signal Conditioning Box” which contains a series of high and low pass filters used to both increase gain in the input MUAP signals and filter out input signal noise. These filtered signals are then digitized by analog to digital converters (commonly known as ADCs) so that the data can be manipulated by the microprocessor. All output data are sent to a client computer via USB cable (after an isolation stage) to be processed further.

4 Electrode Encasement Design Options

Previous EMG acquisition systems included a simple electrode bolt to wire connection which later was introduced to electronics to help amplify the signal. This style of design required long wires before the amplifier, resulting in possible insertion of noise. This project tried to improve on previous designs by including an instrumentation amplifier inside the casing for the electrode bolts. This encasement style has a smaller profile than the active electrode-amplifier from the 2005 system. Also included in the encasement design was a capacitor in series with the gain setting resistor in the instrumentation amplifier, leading to a high pass characteristic while still contributing gain. The high pass characteristics results in DC of 1 between the two electrodes, meaning that the signal that is amplified will be close to purely differential.

The amplifier also incorporates a fixed pass band gain of 50 V/V, allowing the signal to be run through long wires without having the effects of induced noise. The instrumentation amplifier chosen for this project is the AD8220 due to its low noise characteristics. The voltage noise chart shown below in Figure 18 from the datasheet describes the voltage noise over frequency with different gain selections. The gain selection chosen for this amplifier leads to an overall voltage noise of roughly 17 nV/√Hz across the frequencies of interest.

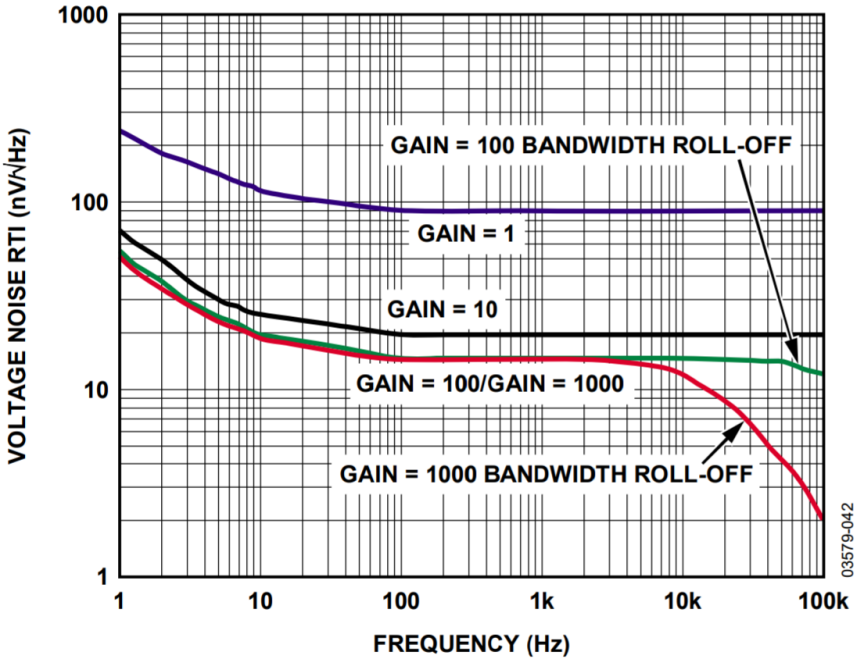

Figure 18: AD8220 Voltage Noise Vs Frequency

One factor also explored in the selection of an instrumentation amplifier was the current noise of the device. This noise can be calculated by multiplying the input impedance of the device by its input bias current. As the AD8220 has a JFET input, the input bias current is only 10 pA according to the datasheet which, combined with its high impedance (listed at 10^4 GΩ), causes very low extra noise added.

Another advantage that this project had over previous iterations was the mounting method of the electrode bolts. Previously, standard nuts and bolts were used which caused the height of the electrode-amplifier package to be very large. The final design of the electrode included modified PEM nuts which will be discussed in further detail later in this report.

The electrode amplifier was also required to be encased in some manner. Encasement prevents human contact with electrical equipment as well as provides durability to the electrode assembly. After several iterations and ideas, the candidate electrode assemblies chosen for this

design were silicone encasement (1), resin encasement (2), and 3D printed encasement with resin filling (3).

4.1 Design Option 1: Silicone Encasement

Overview:

The silicone encasement idea stemmed from the fact that users of the EMG acquisition device will possibly be wearing the electrodes for long periods of time and comfort or irritation may be an issue with alternative materials. Silicone provides a slight grip to the skin while being water repellent and electrically isolating.

The finished product of the design can be seen below in Figure 19.

Figure 19: Silicone Encasement

This design had the advantage of being the slimmest design of the models tested, however, due to silicone flexibility, it suffered from lack of durability. If alternative silicone was used, there could have been a stiffer silicone that would have provided the comfort of silicone with the durability necessary for repeated flexing of the case over many years. A side view shows the thickness of this option below with roughly only 4.8 mm of height (not including the

protruding bolt heads). The total dimensions of the body are 3.18 cm tall x 0.48 cm thick x 1.14 cm wide.

Figure 20: Silicone Encasement Side View

Detailed Assembly:

In order to create this thin silicone encasement, a 3D model was created using Dassault Systèmes' SolidWorks (a common 3D modelling CAD software package). This design shown below was the result of several different revisions. Most of the previous silicone encasement styles had bolt heads facing upwards out of the open-face mold which resulted in part of the bolts being covered with the encasement material. As electrode surface area is important to create good electrical contact, the design was modified in order to allow the bolts to be seated facing downward in a mold, where the silicone would be poured into the mold and then any excess silicone curing over the bolts was cut away afterwards.

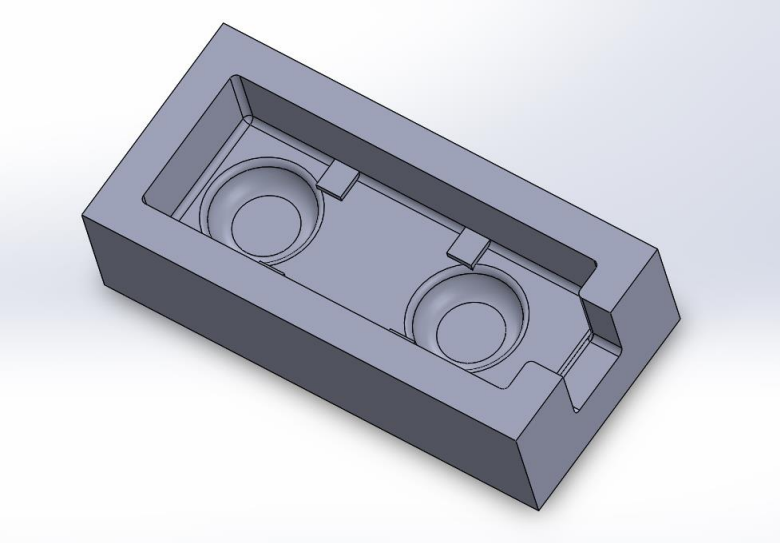

Figure 21: 3D Printed Mold with Head Holes

The figure below shows how the assembled PCB body, with the bolts secured to the circuit board, should be lowered into the mold.

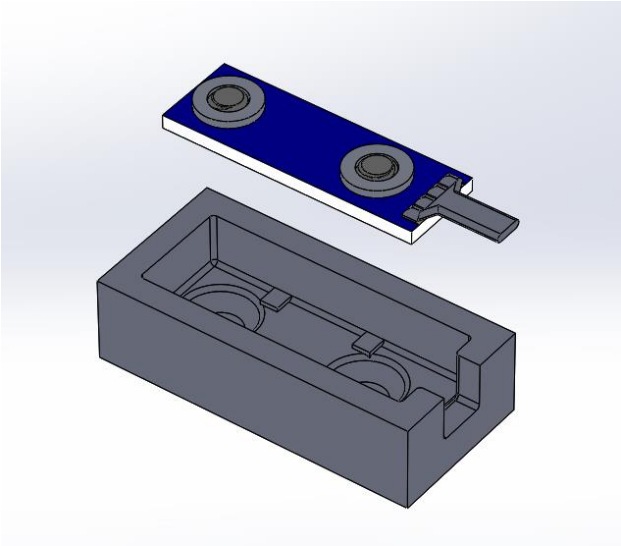

Figure 22: 3D Printed Assembly for Silicone

A cross-section view in the figure below shows the small amount of gap between the board/bolt heads and the 3D printed mold. This space is created due to the mold's standoff rectangular blocks that hold up the board, allowing silicone to flow under the board.

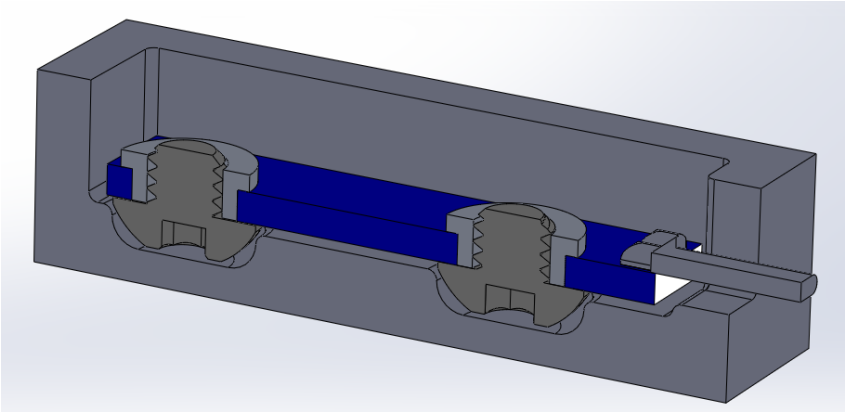

Figure 23: Silicone Cross Section View

Once the model file is acquired and saved as a .STL file, it can be loaded into a "slicer" program which will allow 3D printers to print the file (note that some files might require repositioning before printing). This particular model can be found at https://www.thingiverse.com/thing:2776036. The model can be printed through various online websites including the site at which the model is hosted. A zip file with all designs can be found at https://www.dropbox.com/s/k0a05hc43at57qq/EMG_MQP_Models.zip?dl=0.

After printing, the model is shown in the figure below.

Figure 24: 3D Printed Silicone Mold

The next step in the encasement process is to solder components and wires to the electrode assembly board as well as mounting the screws and modified PEM nuts.

Electrode Mounting and Wiring

One of the main concerns of using a traditional nut to keep the electrode bolt in place was that the overall profile of each electrode pair would be thicker (due to the large profile of the nut) PEM engineering manufactures many different kinds of standoffs and nuts that are designed to embed into different materials. The PFLA-832-1 is a press fit nut that was designed for plastics and comes in aluminum and brass versions. The aluminum versions were used for better conductivity. Figure 25 below shows an unmodified PFLA-832-1 nut.

Figure 25: An Aluminum PFLA-832-1 Nut

Although the threading and size of the nut is ideal, the overall height of the insert is too long for a standard 1.6 mm PCB. Each PFLA-832-1 nut was modified in order to be used in the electrode assembly.

First, the side flanges were removed. The flanges were removed by using a flat head screwdriver and a pair of diagonal cutters to pry each flange off at the base. Initially, the flat head screwdriver is placed through the opening at the top of the nut while diagonal cutters are used to remove one side flange as shown in Figure 26. Once the first flange piece is removed, the base of the nut can be gripped with a pair of needle nose pliers while the remaining flange is removed with diagonal cutters as shown in Figure 27.

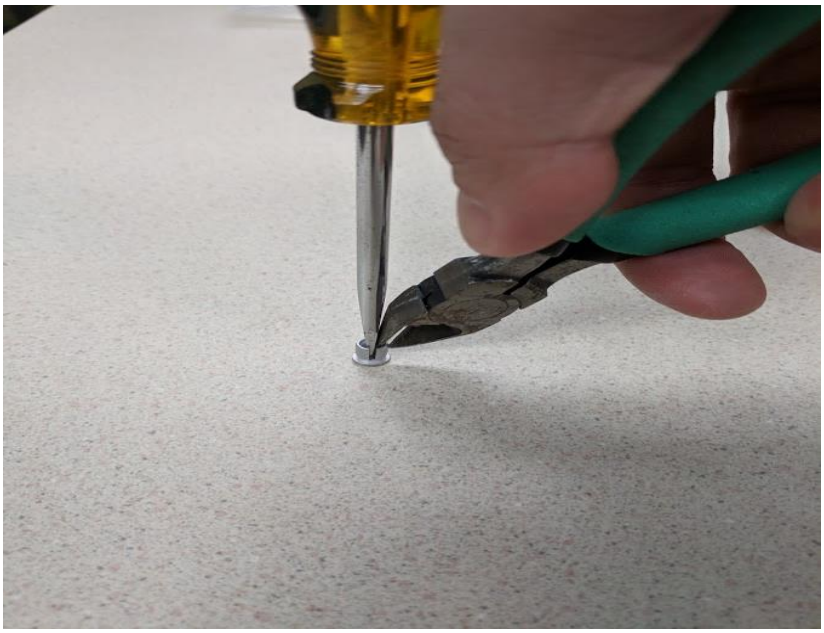

Figure 26: Using a Flat Head Screwdriver and Diagonal Cutter to Remove a Flange.

Figure 27: Using a Pair of Pliers to Help Remove the Second Flange

After the flanges were removed, a file was used to grind opposite sides of the nut. Grinding is performed until there is ample grip with the pliers (roughly 3 mm from any edge in this case) and ensures a good position for the pliers to grasp while the bolt is installed. Figure 28 below shows the modified PEM nut.

Figure 28: Modified PEM Nut

With the electrode assembly in a vice, pliers are used to grip the modified nut while the bolt is screwed from the other side using a screwdriver. Figures 29 - 30 show this installation.

Figure 29: Using a Pair of Pliers to Grip the Modified Nut

Figure 30: While Gripping the Nut with the Pliers, use a Screwdriver to Tighten the Bolt

This operation is then performed to the other bolt. Next, the channel wire is soldered to both the board and the Micro USB B connector. The NMUF 4/30-4046SJ from Cooner Wire is a 4 wire cable with braided shield wire. Each wire is 30 AWG and advertised as an ultra-flexible wire. The electrode PCB wiring orientation is shown in Figure 31.

Figure 31: Top View of Electrode PCB with Wiring (from left: red, green, black, white)

On the connector side, the wire orientation is shown in Figures 32-33 below.

Figure 32: Bottom Side Wiring (Shield: GND and Red Wire: 3.3 V)

Figure 33: Top Side Wiring (White: -3.3 V, Green: SIGNAL, and Black: GND Wires)

After each wire is soldered to the connector, hot glue is applied to the connector encasement to provide strain relief and durability. Figures 34-36 illustrates this process.

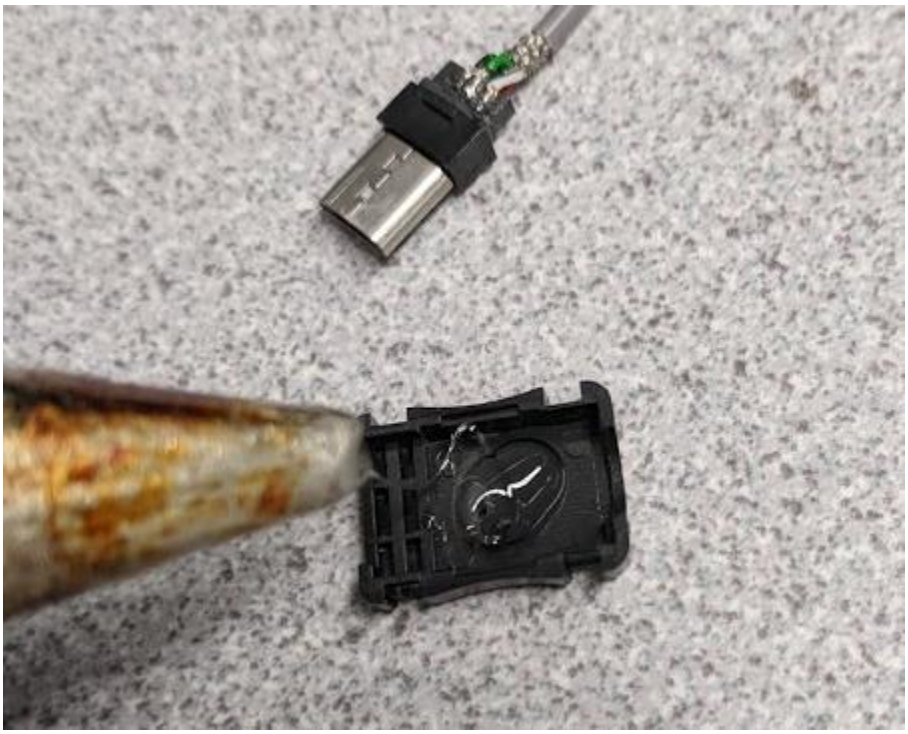

Figure 34: Hot Glue Applied to the Bottom of the Connector

Figure 35: Micro USB B Connector Placed on Top of Hot Glue

Figure 36: Hot Glue Applied on Top of the Connector Before Full Encasement

Before completing the micro USB connection, be sure to add a small length of heat shrink tubing in order to provide strain relief to the base of the electrode assembly encasement.

Once the strain relief is provided, the assembly of one channel is complete. Once it is tested for functionality, each board is encased.

Silicone Molding

Once these steps are completed, the silicone is ready to be mixed and poured. The silicone used for this project is OOMOO™ 30, an easy-to-use silicone that only requires the user to mix equal parts of A and B compounds by volume in a cup, pour into the mold, and let sit. After mixing, our team found success in using a 10 mL syringe to fill the base of the mold before dropping the PCB in, reducing the risk of air bubbles in the mixture. Once the PCB was in place, additional silicone was poured on top in order to fully cover the electronics. A picture of the filled silicone mold is shown below. Note that a piece of tape could have been used around the wire at the base to hold more silicone in the mold, however, the extended section is used for strain relief only and silicone cleans up easily.

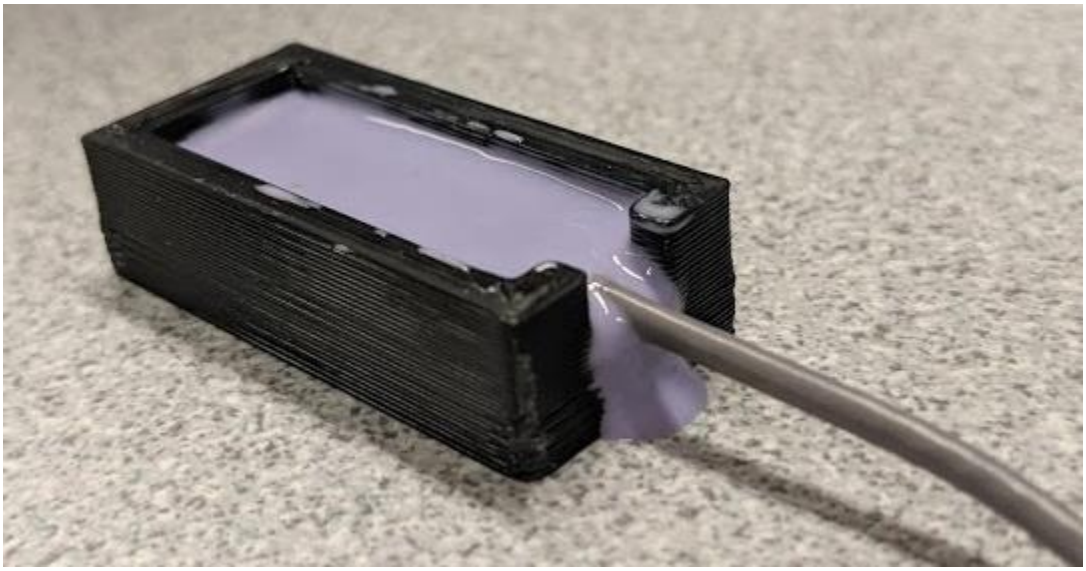

Figure 37: Silicone Mold Poured

When the mold dries, simply remove the silicone encased board from the mold and trim excess silicone with a razor blade.

Figure 38: Covered Silicone Mold Before Trimming

4.2 Design option 2: Resin Encasement

The second design option is a resin encasement. This specific design option includes a few steps the first time that it is performed but will result in an easy to make mold that can be reused. The final result of this encasement style is shown below. Note that the consistency of this design is not perfect. We found it hard to control the amount of material applied to the top surface without covering the electrode heads. The total dimensions of this design were 3.18 cm x 1.27 cm x 0.55 cm.

Figure 39: Untrimmed Resin Encased Electrode

This design option allows for a hard encasement that will be very resistant to component damage. It is larger than the silicone mold as there is not an easy way to remove excess resin if the bolt heads were covered.

The first step in the process to create a resin encasement is to 3D model and print the negative. The latest design of this can be found at https://www.thingiverse.com/thing:2776054. All model files can be downloaded in one zip file through the following link: https://www.dropbox.com/s/k0a05hc43at57qq/EMG_MQP_Models.zip?dl=0. The printed model should be identical to the piece in the figure below.

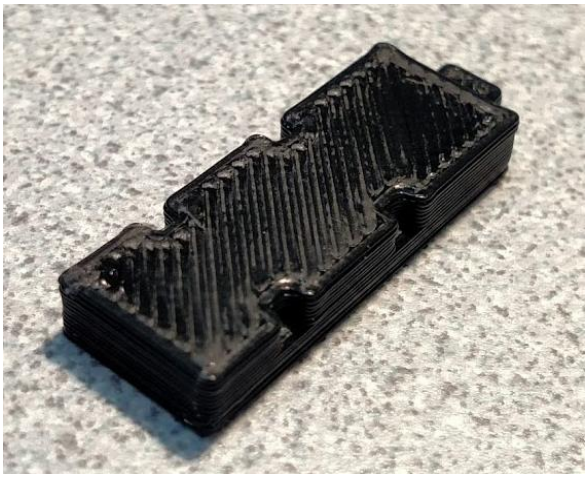

Figure 40: Resin Encasement Negative

Once this piece is printed, a silicone enclosure will have to be created in order to make a silicone mold into which resin will be poured. Our team created the enclosure with pieces of cardboard and hot glue as shown in Figure 46 below with a five-sided cardboard enclosure. The 3D printed piece should be set up against the edge of one of the walls in such a way that the wire exit can be placed perpendicular to and touching a wall as shown in Figure 41. Note that the negative should be placed with the indentions facing upwards as in Figure 41. Once the negative is placed, silicone should be mixed and poured to cover the piece. Note that the height of poured liquid should be at least double the height of the 3D printed mold to ensure that the silicone doesn't break.

Figure 41: Cardboard Enclosure

Figure 42: Poured Silicone Mold

After removing the cardboard enclosure and flipping the silicone top to bottom, as well as the 3D printed piece, the silicone enclosure should look as shown in Figure 43.

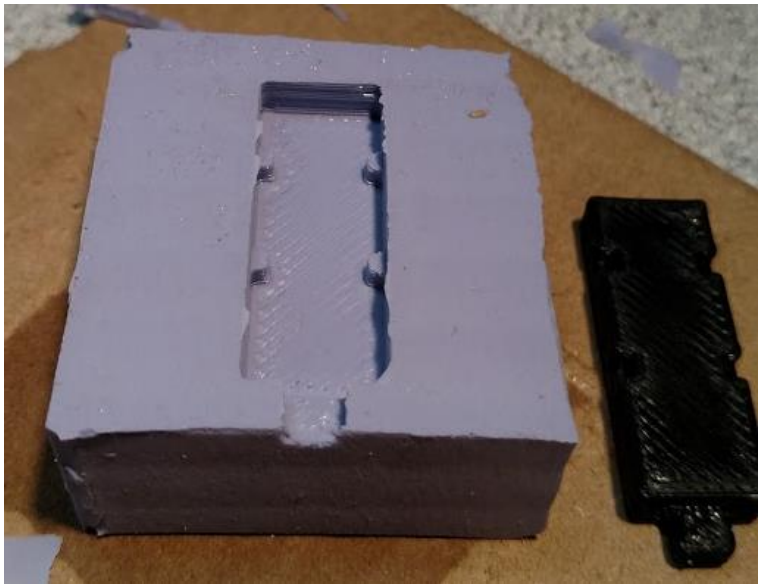

Figure 43: Silicone Mold

Once the electrode assembly PCB is assembled with wires, electrical components, and bolts, a syringe is used with a resin in order to fill the mold and top of board with resin. Our group used Smooth-Cast 300 Liquid Plastic resin, a simple 1:1 ratio resin with low viscosity. The result is shown in the figure below. Note that the resin pours clear and dries white after a short time. When the resin hardens, the encased electrode is removed and trimmed and a new electrode can be put in the mold again to be filled with resin.

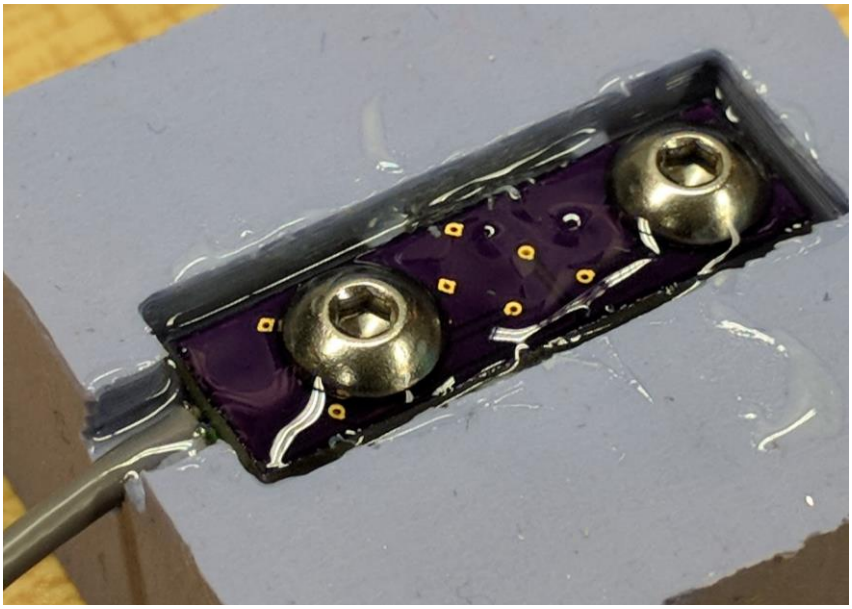

Figure 44: Resin in Mold

4.3 Design Option 3: 3D Printed Case Filled with Resin

The last design option is a 3D printed encasement that surrounds the PCB. When inserted, there is a cavity holding the electronics and nuts, shown in Figures 45-47 below.

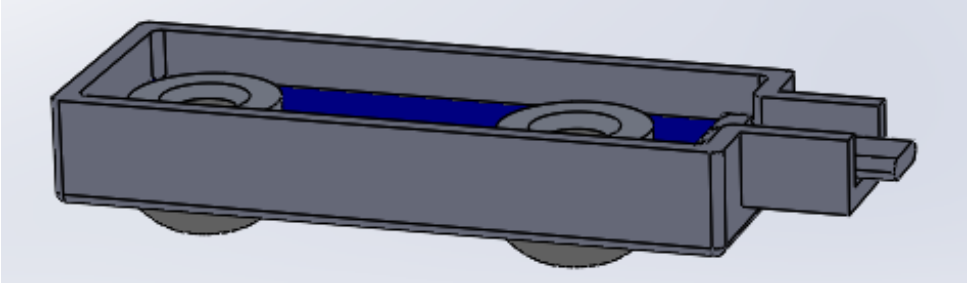

Figure 45: Design Option #3 Model

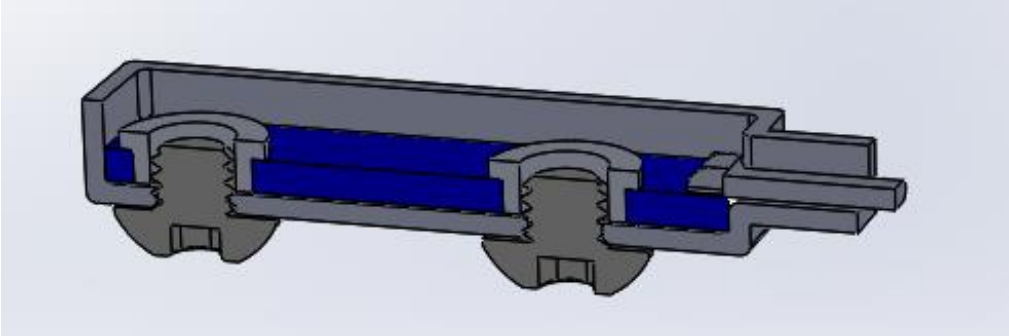

Figure 46: Design Option #3 Cross Section

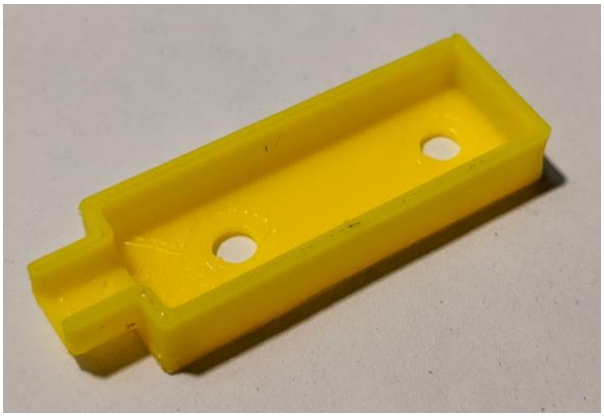

Figure 47: 3D Printed Encasement

Once the models which can be found at https://www.thingiverse.com/thing:2774269 or https://www.dropbox.com/s/k0a05hc43at57qq/EMG_MQP_Models.zip?dl=0 is printed, the soldered electrode body (without the bolts) is inserted into the encasement and the bolts are

threaded from the outside. The bolts and nuts secure the circuit board in place within the case. The bolt side of the encasement will rest on the table flat, while the circuitry side faces upwards. When the device is assembled, the body is stabilized and the resin is poured with a 10 mm oral syringe until covered (as the bolt heads on the bottom are round and make it hard to pour resin). This process is shown in Figure 48 below.

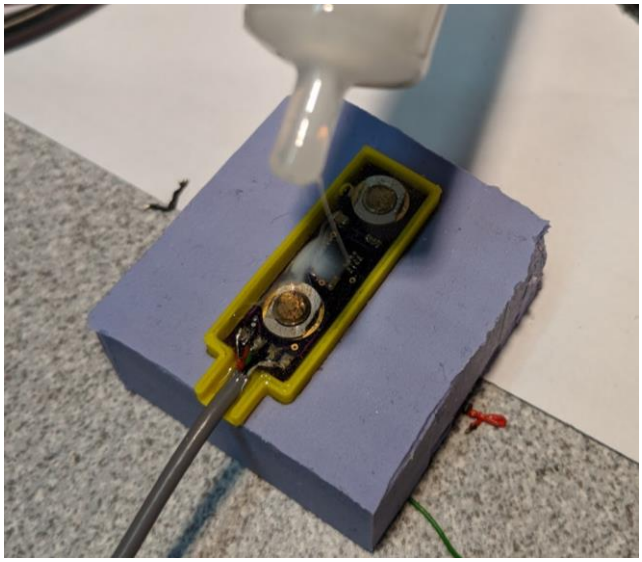

Figure 48: Mold Sits on a Pad to Keep it in Place While Resin is Poured

The resin is left to dry (the cure time according to the box is at least 10 minutes). The final result is shown in Figures 49-50 below. Note that the brass bolts used in this diagram were for demonstration purposes only. Stainless steel bolts are used on the final encasement design. The final dimensions of this design is 3.18 cm tall x 1.19 cm wide x 0.51 cm thick.

Figure 49: Final Backside of 3D Encasement

Figure 50: Top Side of 3D Encasement

4.4 Electrode Encasement Design Option Selection

Overall, the durability limitations of the silicone encasement and the non-uniformity and repeatability of the resin encasement led the team to choose the 3D encasement with resin filling as the final design option for the electrode. This design option (Design Option 3), proved to be easy to make as well as rugged and still relatively thin.

Figures 51-52 below shows the electrode design option #3 side by side with previous electrode designs.

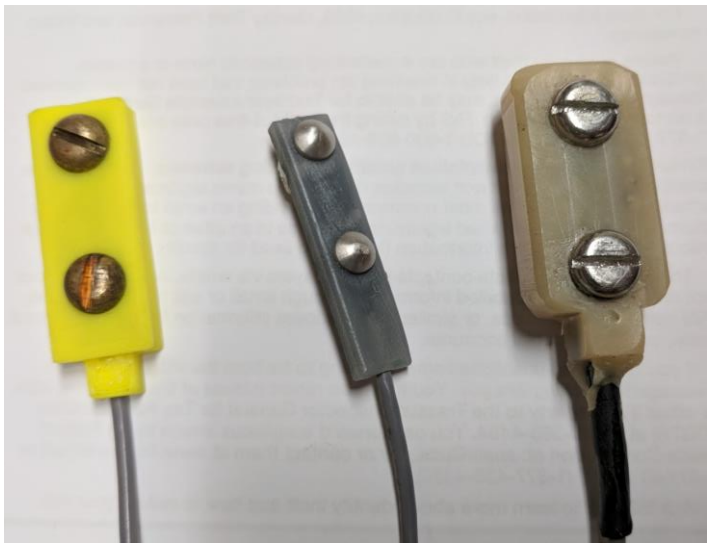

Figure 51: Top view of electrode versions (from right: 2002, 2015, 2018)

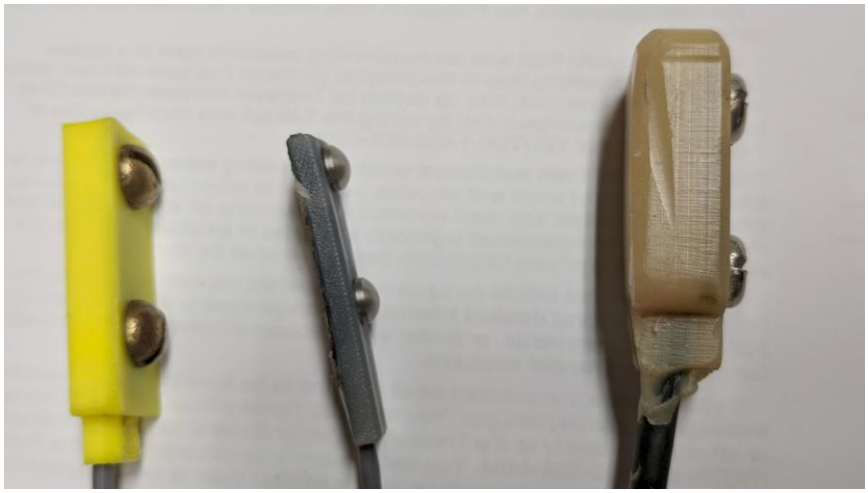

Figure 52: Side view of electrode versions (from right: 2002, 2015, 2018)

5 Signal Conditioning Box Design Options

To design and build an EMG which fulfilled all of our detailed design specifications, four different design options were considered and evaluated. Each design option details electrical topographies as well as advantages and disadvantages in comparison to each other.

Several design optimizations will also be included in several of our design options. Filtering is a very important part of signal processing. In hardware, changes to filters take time, effort, and money. In software, filter changes can be made on the fly in a small amount of time. Therefore, for the best possible solution, the design options considered should be able to accommodate software filtering. Generally, 16 bits is considered great resolution but a 24-bit system is required for use in this proje7ct as it allows for 16 bits of resolution as well as a few bits for high pass filtering and 3-5 bits of software gain. Noise in the system will be generated about the 0 V line, meaning that the small amount of noise generated by the ADC will only take up the first few levels of the ADC. If one were to index the bits of the output from bit 3 to bit 23, there will be 21 usable bits of the system. If only 16 bits were required, one could index from bit 3 to bit 20 and then have 3 bits of software gain as shifting the array to select from bit 4 to 21 and using 16-bit conversion to get back the original voltage level will result in a gain of 2. This process can be performed again twice, resulting in a total possible gain of 2^3=8 for 3 bits. As stated earlier, the selectable gain levels must be 1, 2, 4, 8, 16, 32, 64 and 128. With a gain of 8 available in software, the system chosen is only required to provide gains of 1, 2, 4, 8, and 16. On another note, some systems may require a low pass filter to avoid aliasing before the ADC so that must be included on the design chosen. A simple RC low pass is all that is required, as sigma delta ADCs (used in this design) actually sample in the MHz range. If a low pass filter is used with a low cutoff such as 5 kHz, an RC filter will be fine.

Also, in previous iterations of this device, gains were set using manual switches on the face of the device. By using the ADS1298 sigma delta converter, we can integrate each channel gain stage into software, eliminating the need for mechanical switches or dials. The gain instead will be set in the graphical user interface on the PC.

5.1 Design Option #1

One design option for this project was to have the signals coming from the electrode assembly filter through a second-order high pass filter on the signal conditioning board using an OPA4170 (Texas Instruments) operational amplifier (commonly referred to as an op-amp) followed by a resistor-capacitor (RC) low pass filter. The designed cutoff frequency for the high pass filter is 10 Hz in order to eliminate noise caused by motion artifacts while the cutoff for the low pass filter is 3978 Hz to remove any high frequency noise and prevent aliasing from the ADC. The filtered signal will be digitized by an ADS1298 ADC from Texas Instruments. The newly digitized signal will be processed by the microprocessor to be sent to the PC. Figure 53 shows the topology of this design option.

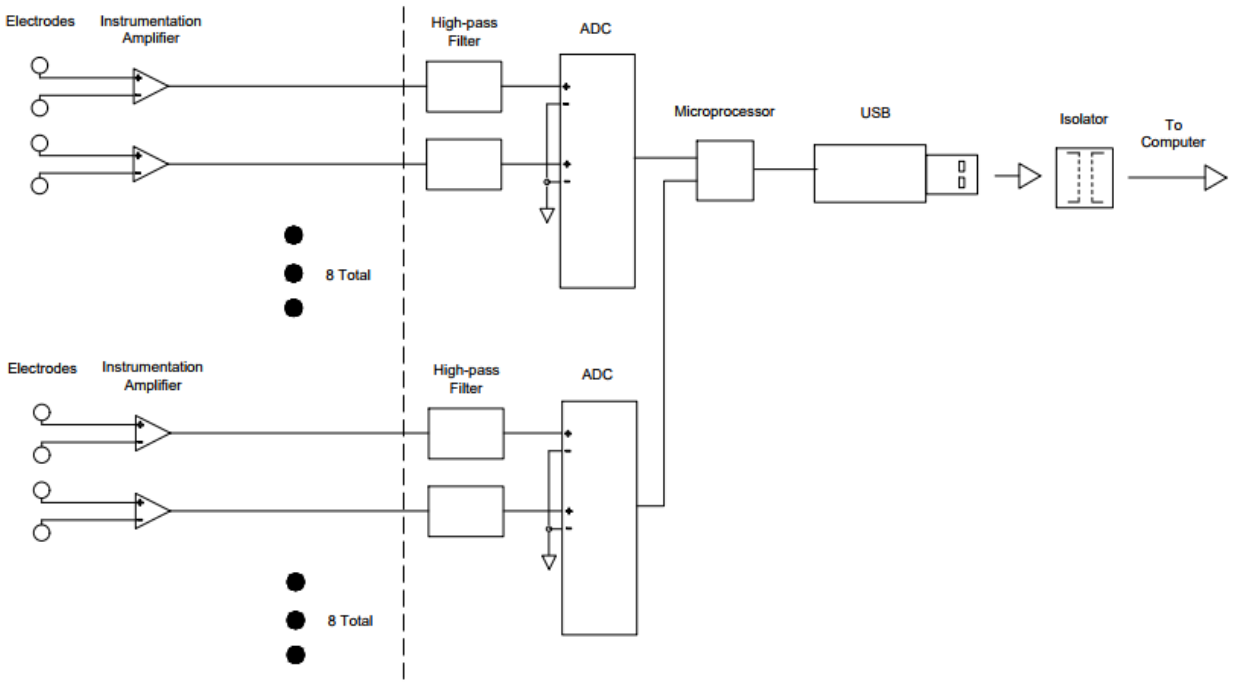

Figure 53: Design Option #1 Topology

The ADS1298 contains 8 differential inputs and internally selectable and programmable gain amplifiers (PGAs) with gains of 1, 2, 3, 4, 6, 8, 12. With only differential inputs, all negative terminals of the input channels will be connected to ground.

Advantages

- With the ADS1298's integrated PGAs, gain can be set directly using a command from the microprocessor without the use of additional components.
- All gain selection can be made in software, eliminating the need to change resistor values after a printed circuit board is created if hardware gain needed to be changed.

Disadvantages

- Proper operation of the ADS1298 is more complex with the included PGAs and application specific inputs and outputs such as right leg drive and heart rate monitor pins.

These additional hardware features mean that the ADS1298 will be more difficult to implement in software.

- The ADS1298 only can be used in 8 differential channel configuration. Therefore, two ADS1298s would be required to implement 16 channels.

5.2 Design Option #2

The second design option uses a 16 channel 24-bit ADC such as the ADS1258 from Texas Instruments, with external PGAs to implement the levels of gain. The PGA LTC6192 from Linear Technology can implement gains of 1, 2, 4, 8, 16, 32, and 64. The PGAs' gain settings would be changed using a digital control signal send by the microcontroller through a digital demultiplexer (deMUX). Figure 54 below shows the topography of the design option.

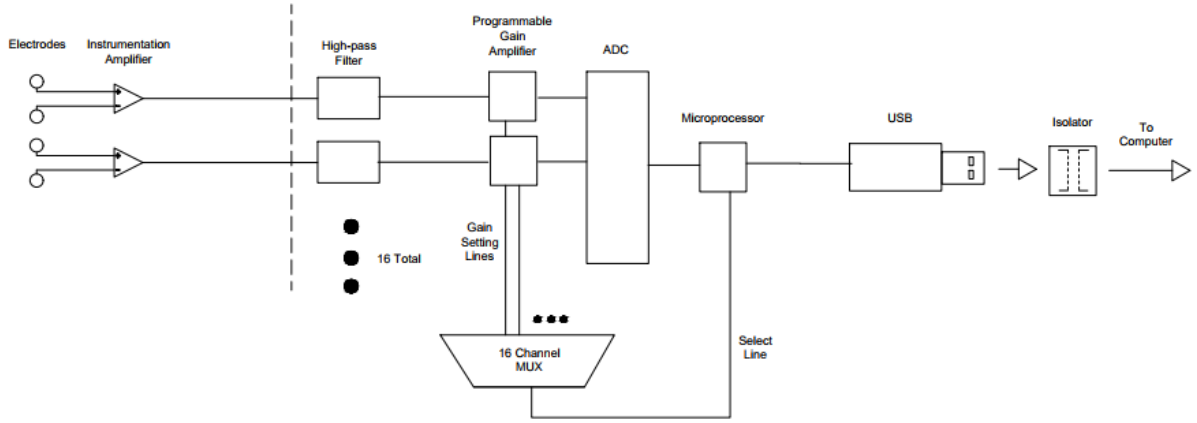

Figure 54: Design Option #2 Topology

The ADS1258 comes in a 16 single ended channel or 8 differential channel configuration. Each PGA would be controlled from the microprocessor by sending a command to the deMUX, which would change the gain of the desired channel. A deMUX is necessary in this case as the microprocessor may have a limited number of communication lines. Similar to Design Option

#1, the output digital signal from the ADC will be processed by the microprocessor and transmitted to the PC.

Advantages

- Software complexity is reduced with a simpler ADC as well as external PGAs controlled by a central deMUX. Levels of gain of individual channels can be changed with simple deMUX switching and PGA commands.
- The ADS1258 can be used in 16 single ended channel configuration. Only one chip would be required to implement all 16 channels.
- The LTC6192 is able to reach high levels of hardware gain, which increases the range in which the 24-bit data can be bit shifted for additional levels of gain.

Disadvantages

- Each LTC6192 PGA contains two individually programmable gain circuits. For 16 channels, a total of 8 chips would be required and significantly increases the number of components required.
- The LTC6192 PGA has a standby supply current draw of 4.5 mA per chip. With 8 chips, the total current draw is 36 mA of current used to power all PGAs.
- The LTC6192 PGA adds considerable noise to the analog signal before the ADC stage.

5.3 Design Option #3

The third design option will use the same instrumentation amplifier and op-amp as the previous design options. The ADS1298 will be used as the ADC, but each electrode input will be split into two channels: one will have with a fixed gain of 1, and the other will with a fixed gain of 16. In conjunction with the ADS1298's internal PGAs, each electrode signal input can be

modified with a gain of 1, 2, 3, 4, 6, 8, 12, 16, 32, 48, 64, 96, 128, and 192 between the two channels. Figure 55 shows the design topology below.

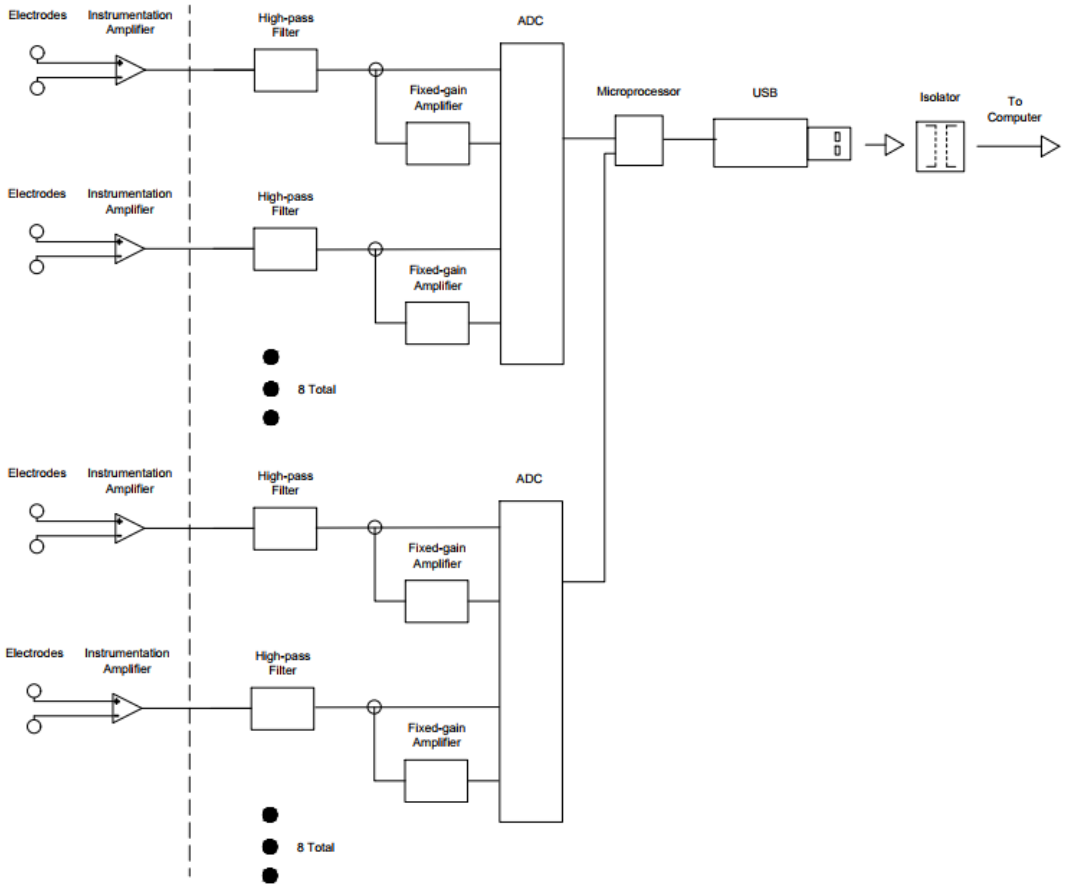

Figure 55: Design Option #3 Topology

With two ADC channels per electrode channel, the microprocessor would be programmed to choose one of the two electrode channels to send to the PC based on the desired gain levels.

Advantages

- By implementing a fixed hardware gain in addition to the ADS1298's integrated PGAs, this design option can achieve very high hardware gain.

Disadvantages

- In order to accommodate twice the number of channels, 4 ADS1298's would have to be used. The increased number of ADCs adds complexity to the software development and may increase the time needed to process all 32 channels of data.
- This design option requires many additional components to implement the fixed hardware gain as well as the additional channels.

5.4 Design Option #4

In our final design option, high precision commercially available ADCs will be used to convert the front end analog inputs to digital outputs that will transmit to the PC. In previous iterations of the wired EMG acquisition system, ADCs from National Instruments such as the PCIe-6361 were connected to the PC motherboard directly. As the previous projects have only been used with 16 bit systems, there is an added challenge in finding a 16 channel 24-bit data acquisition unit. One such device is the DT9826 from Measurement Computing, which provides isolation, high enough sampling rates and more, but comes at a cost of 2750 USD.

Figure 56: Design Option #4 ("DT9826 Series.")

The system diagram for this design option is shown in Figure 57 below. The system includes sixteen electrode assemblies, a custom adapter board, the DT9826 unit, a medically

isolated power supply, and a USB connection. Note that a custom adapter board must be used in this option as the electrode assemblies currently have power running to the units, not provided by a BNC input. The adapter board would allow the signals to be routed to the inputs of the DT9826 as well as receive power from the Digital I/O. Voltages will have to be regulated and inverted in order to supply the correct power to the electrode assemblies.

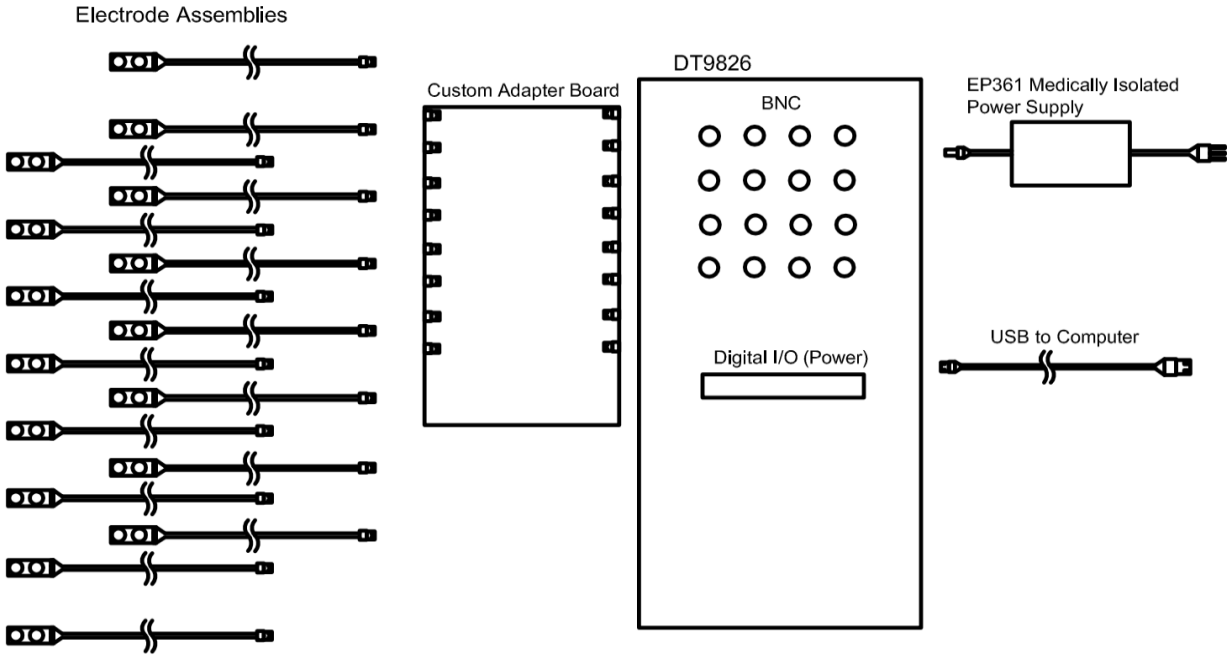

Figure 57: DT9826 Series System Level Diagram

Advantages

- Each ADC unit from Measurement Computing has high precision and fast sampling rates with integrated noise filters to ensure accurate data acquisition. These ADC systems would be able to perform better than the current single chip solutions such as the ADS1298 and ADS1258.

- Commercial ADCs would be purchased pre-built, and can be used immediately and without the need of additional software development to interface with MATLAB or other similar programs.

Disadvantages

- High precision ADC solutions are very costly. As previously mentioned, the DT9826 costs 2750 USD and adds immense cost to the device.
- This device would require adaptation in order to power the electrodes as well as receive signals.

6 Final Design

6.1 Overall Comparison

Due to the enormous cost of Design Option #4 (professional data acquisition card), it was eliminated immediately. Design Option #2 (using external PGAs) was eliminated due to the requirement for a large amount of hardware necessary and the current required to run these devices. Design Option #3 (hardware gain of one and sixteen) would have allowed for higher resolution of small signals, however, it required two inputs for every channel. The additional inputs would have been acceptable if an ADC such as the ADS1258 was used due to the feature of single ended inputs. However, after deeper research was performed, the ADS1258 was incapable of acquiring the data from all 16 channels at the rates necessary for this project and would have produced aliasing for signals at 1800 Hz. If an ADS1298 was used instead of the ADS1258 in Design Option #3, there would have been a large number of gains selectable by the user, however, as the ADS1298 is purely differential (not single-ended) it requires twice the amount of input channels and thus requires twice the amount of chips for 16 channels. The ADS1298 also has internal programmable gain, and does not need two hardware gain stages. An additional consideration of Design Options 1-3 was the addition of an embedded ADC, leading to a small size and cost in comparison to the large and costly desktop solution of Design Option #4. Due to the impact of the ADS1298 on board space and cost to the overall project, Design Option #3 was eliminated and Design Option #1 was chosen as the final design option. A table summarizes the considerations below. The noise figures were estimated from voltage noise charts in the respective datasheets. The voltage noise was estimated based on a flat-line approximation of the voltage noise for the specific gain levels required for the instrumentation amplifier over a frequency range of 20-1800 Hz. Note that the cost for design options 1-3 only

includes the components required for the filters and sampling, not the cost of additional necessary equipment such as PCB fabrication, microcontrollers, power converters, and electrodes.

Table 2: Design Options Summary

Design Option	Current	Cost	Voltage Noise (RMS RTI)	Size	Weight/Mobility
1	60mA+	$210+	0.63 uV	Small	Mobile
2	140mA+	$190+	0.55 uV	Small	Mobile
3	80mA+	$190+	0.55 uV	Small	Mobile
4	Unspecified, requires power supply	$2750+	Unspecified	Large	Desktop Unit

6.2 Design Optimum Selection

Design Option #1 was chosen as the final design for several reasons. Using only two ADCs for 16 channels accompanied with a fixed front end gain and adjustable PGAs inside of the ADS1298s yielded the fewest required components while reaching our minimum requirements for our finished design. As shown in Table 2, Design Option #1 consumes only 60 mA for all 16 channels up to the ADC while staying at a comparable cost level. On the software development side, this design option provides the least programming complexity of all other

design options. Although the channel voltage noise RMS on average was slightly higher, it was deemed to be within acceptable parameters.

7 System PCB Design

7.1 Electrode PCB Design

The electrode PCB consists of two holes at each end for PEM nuts and electrodes and one instrumentation amplifier with accompanying peripheral components. The PCB layout and schematic is shown in Figure 58-59.

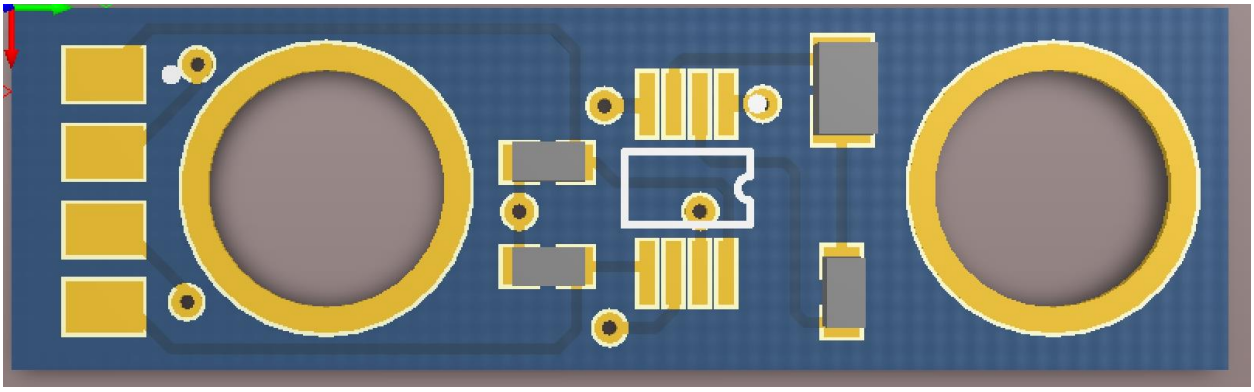

Figure 58: Top Layer of Electrode PCB Board

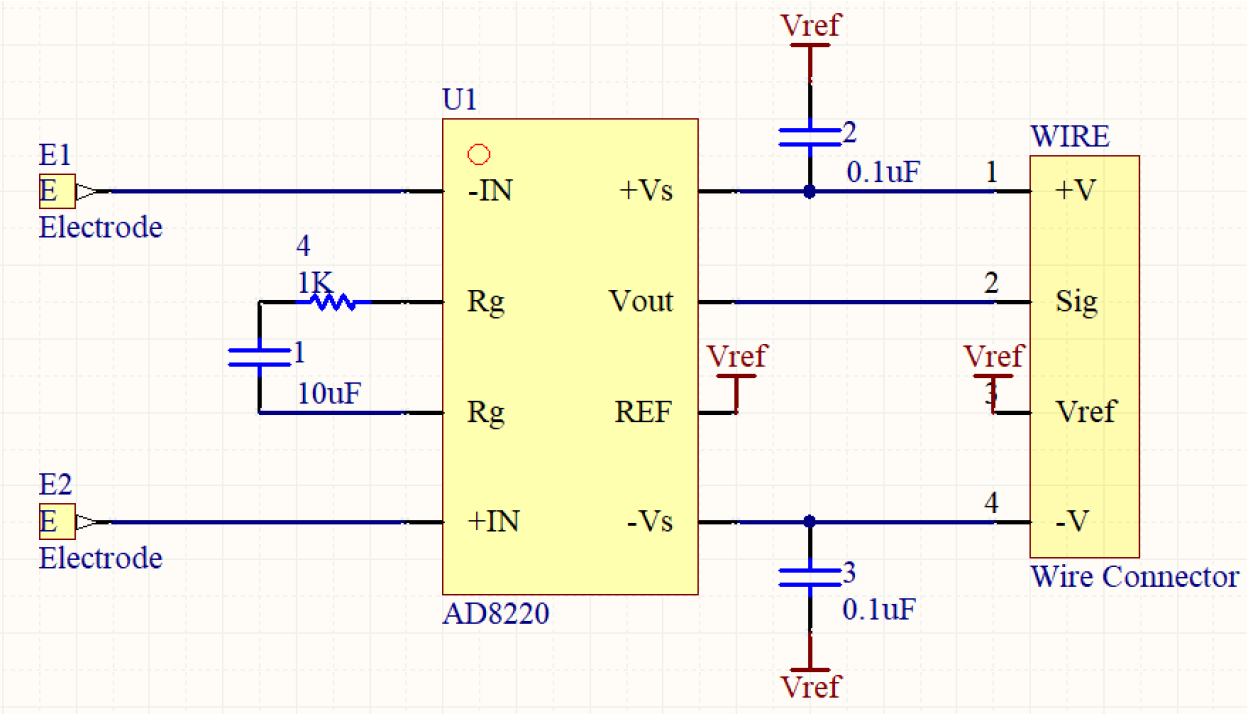

Figure 59: Electrode PCB Schematic

The instrumentation amplifier requires a cutoff capacitor and a gain setting resistor. There are also two bypass capacitors to settle high frequency noise on voltage rails. Four pads seen on the left of Figure 58 are used to solder the wires from the electrode PCB to the main board.

7.2 Peripheral Board

An additional board was designed for channel inputs. Each electrode-amplifier channel plugs into the peripheral board via a micro USB B connector. Eight of these connectors are on each of these two level boards. Standard male jumper pins are used on the bottom side of the board to transfer rail voltages to the instrumental amplifiers on each electrode channel as well as signal pins for input into the main board.

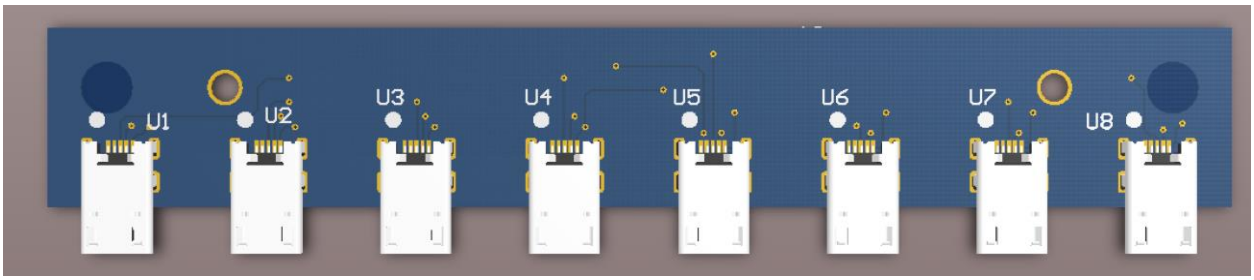

Figure 60: Top Layer of Peripheral Board

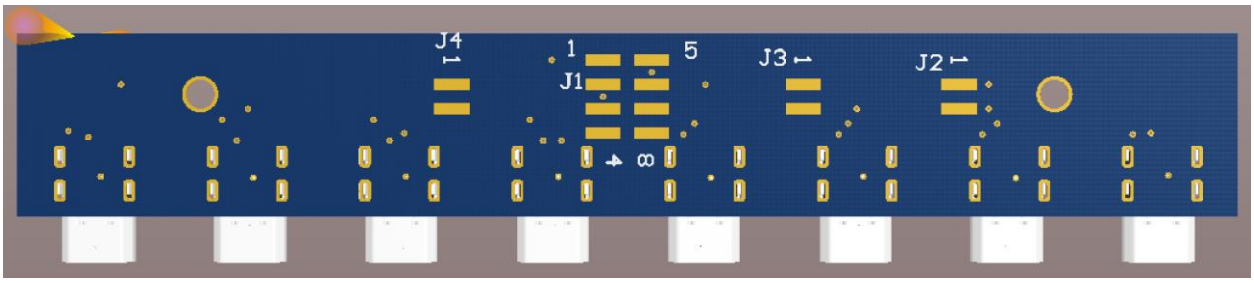

Figure 61: Bottom Layer of Peripheral board

With all three boards attached together, the final dimensions of the EMG device is 5”x3”x4”.

7.3 Signal Processing PCB

The EMG signal acquisition board was ultimately designed and implemented as a Printed Circuit Board (PCB). The board was designed in Altium Designer and consisted of 4 layers shown in Figure 60 below.

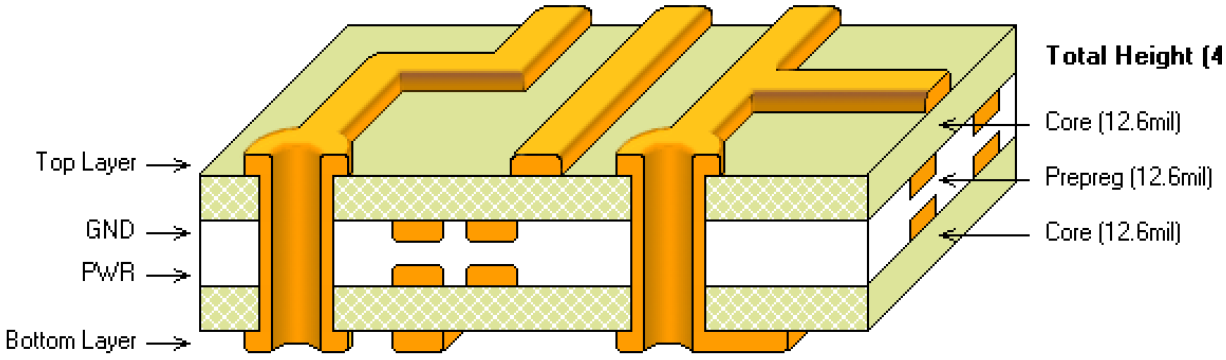

Figure 62: Layer design of the EMG main board

The total dimensions of the main board were 5” x 3” x 0.063” without components installed. With the required electrode amplifier adapter boards (described later), the total dimensions are roughly 5” x 3” x 4”. The component placement was designed with ease of manufacturing and signal integrity in mind. All integrated circuits (ICs) were placed on the top level shown in Figure 63.

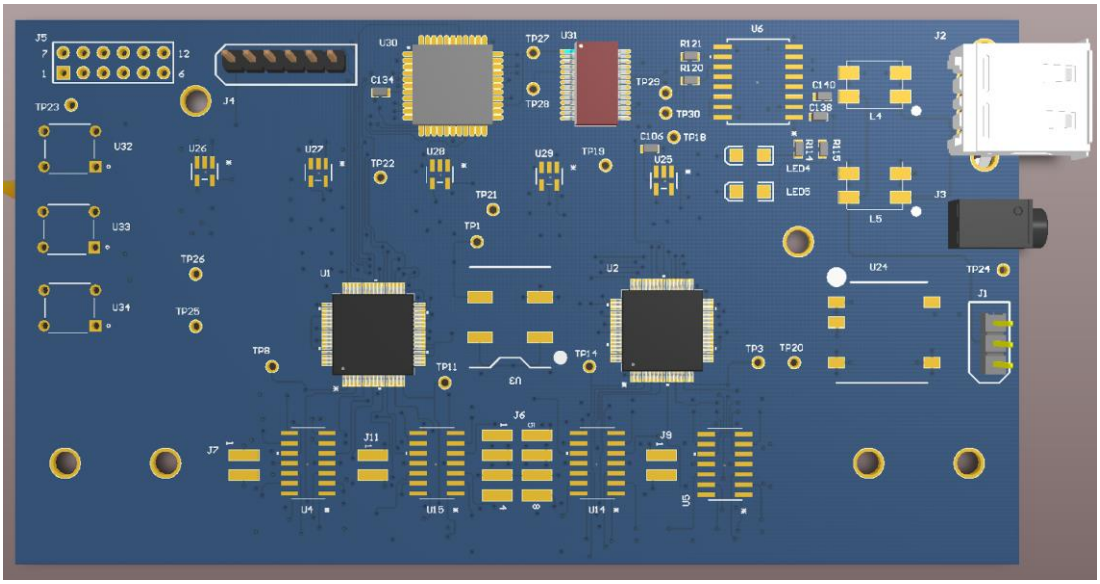

Figure 63: Top Level of Main Board

All resistors, capacitors, and inductors were placed on the bottom level so that if any repairs were needed, components could be easily removed without risk of damaging other components. The bottom side of the board is shown below in Figure 64.

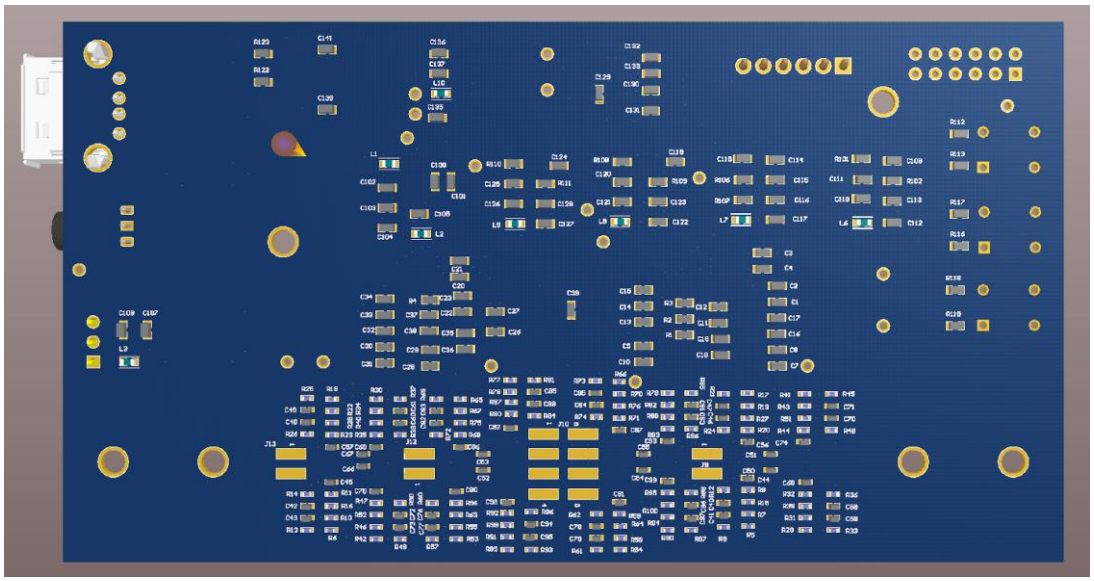

Figure 64: Bottom Layer of Main Board

In order to preserve signal integrity and reduce possibilities of electronic interference, the GND layer was split into power ground (PGND), signal ground (SGND), and analog ground (AGND). Common chokes (essentially inductors) were used to connect each ground to the ground of the USB connector of the computer, which would eliminate high frequency noise and protect sensitive analog signals from electromagnetic interference from sources such as the power line. All analog traces and components were placed away from the signal traces. The separation removes possible electromagnetic interference that could influence sensitive analog components such as the ADC inputs. All components used are detailed in the bill of materials in Appendix A.

Some additional features were also added to the main board design in order to expand functionality. Three buttons, and a 12 pin female connector were implemented. One button was dedicated to the microcontroller reset, while the other two are connected to general I/O ports on the microcontroller and can be used for expanded functionality. Each pin on the connector connects to an unused pin on the microcontroller for potential future use.

8 Software Development

In order to have a working product, software development is also a key part of the project. The project team developed software for both the microcontroller and computer to communicate with the ADCs and control device operations.

8.1 Microcontroller

The microcontroller acts as an interface between the ADS1298 ADCs and the personal computer. The microcontroller's main purpose is to communicate with the ADS1298s, output data to the computer, and accept commands from the computer to change various settings. To perform necessary tasks, the project team developed a program in C language with MPLAB X Integrated Development Environment (IDE), which is the dedicated software development program for the chosen microprocessor, PIC24FJ128GA204. The program is divided into several small modules. Each module has different functions to support the overall operation of the program.

8.1.1 System Configuration

The system configuration is separated into two parts. The first part is responsible for setting system clock rates, and setting of the watchdog clock rate. The code can be generated through the Configuration Bits window in the MPLAB X IDE. Each line of the code has the format that starts with “#pragma config”. The segment of the code needs to be placed before the main function in the main C source file, because these settings need to be executed before the program starts. For this project, the microcontroller uses the default low-power internal oscillator with a frequency of 8 MHz. The microcontroller clock speed was increased to 32 MHz using a

four times phase locked loop (PLL). These settings are implemented through the first part of the system configuration.

The second part of the system configuration mainly focuses on mapping available microcontroller pins for different modules. The pins that are used for digital I/O are set to digital pins. Corresponding registers are also configured to assign different functions for the pins. A register that affects the low-power internal oscillator and the PLL is also configured. The second part of the system configuration is implemented with a function in a separate C source file.

8.1.2 Timer

Certain program modules require time delays in between different code executions. Timer 2 from the timer modules is implemented in a separate C source file to provide the interrupt necessary for the delay function implementation. Timer 2 uses the low-power internal oscillator as the clock source. The interrupt is called at a frequency of 200 kHz. The delay function uses clock count increment in the interrupt to determine the delay time.

8.1.3 Serial Peripheral Interface

The microcontroller uses serial peripheral interface (SPI) to communicate with two ADS1298s. The SPI module is implemented in a separate C source file. According to the ADS1298 datasheet, the shared clock (SCLK) idle stat should be low, the data from ADS1298 are shifted out on the rising edge of SCLK, ADS1298 latches data on the data input pin (DIN) on the falling edge of SCLK. To establish successful communication among devices, the microcontroller SPI module is set to match the SPI characteristics described in the ADS1298

datasheet. A 16 MHz SCLK is configured to provide the fastest data exchange speed. Since the ADS1298 data package size is 24 bits, the SPI data bus size is set to 8 bits, instead of 16 bits or 32 bits. Using a 16-bit or 24-bit data bus would result in data package mismatch. The SPI modules use two chip selection (CS) pins to select which ADS1298 to talk to. Thus, the two ADS1298s are able to share the digital data lines.

8.1.4 Universal Asynchronous Receiver Transmitter

Universal Asynchronous Receiver Transmitter (UART) is the communication protocol implemented to establish the communication between the microcontroller and the computer. The data bus is set to 8 bits, with additional 1 stop bit, no parity. The UART module uses high speed mode, which allows a high speed baud rate. The implemented baud rate for the program is 128000 bits per second. The UART module also has its own interrupt, which is called when an 8-bit package is ready in the data buffer.

8.1.5 ADS1298 Module

A separate C source file is used to implement and group the functions used to control ADS1298s. These functions execute the ADS1298 power up sequence, verify digital communications, change channel gains, write and read from ADS1298 registers, send commands, and update data. Among all these functions, the most important one is the data updating function. The data updating function listens to a flag variable that is set by an external interrupt, which is triggered by the data ready pin from the ADS1298. When there are data ready,

the function starts to call SPI functions to retrieve the status and channel data in an 8-bit package, and reassemble them into 24-bit data.

According to the ADS1298 datasheet, if the SCLK speed is above a certain limit, a delay is needed in between each command sent to the ADS1298. The 16 MHz SCLK used in the program is much faster than the limit. Therefore, the delay function is inserted in between command sending functions.

8.1.6 Main Function

Figure 65 shows the flowchart of the main function operation. The program executes the main function when the program starts to run. The main processing loop of the main function is a three-state machine. Within this state machine, various functions from different modules are called. In the first state, the program polling command from the computer client determines the desired number of samples from an ADS1298. After the sample number is set, the state program enters the second state and issues the command to start the sampling process. Once the start command is received, the program pulls the determined number of samples from all sixteen channels of the ADS1298s. These sample data are sent to the computer client through the UART and the UART-to-USB converter in the third state. All flags and variables are also reset in the third state. Thus, a complete cycle is completed. The state machine is set to the first state again after the third state.

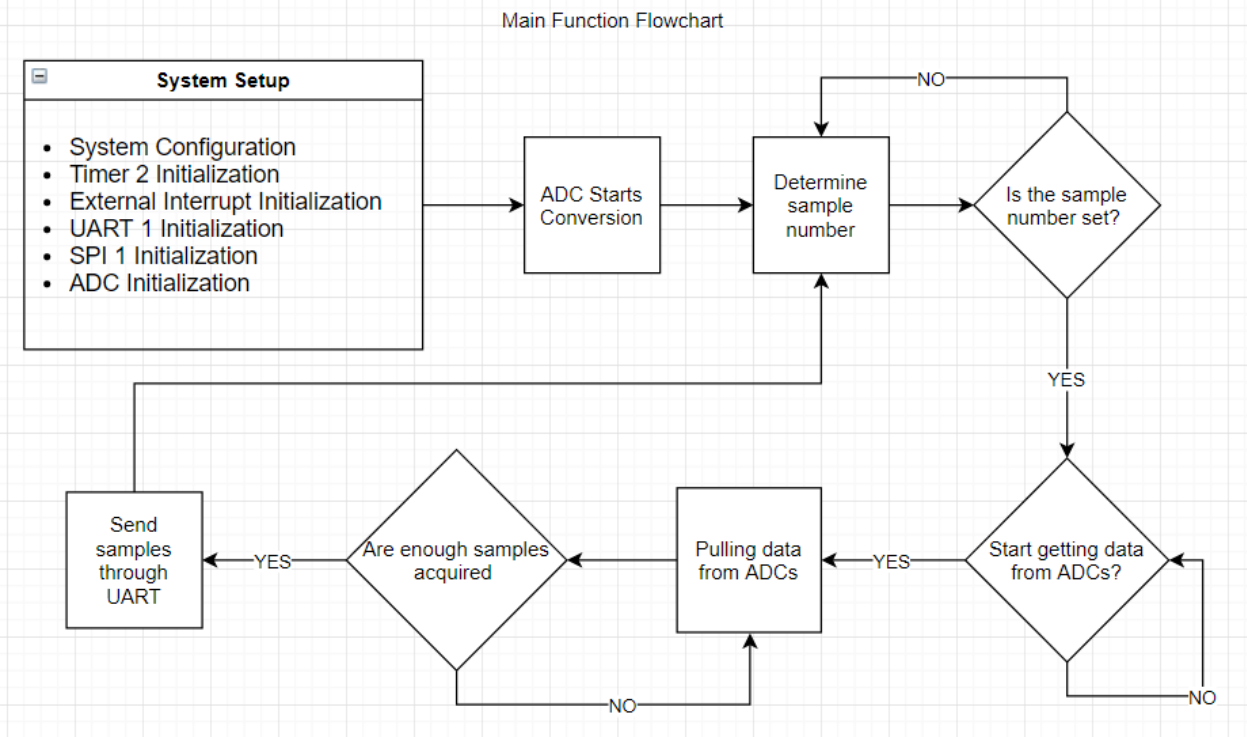

Figure 65: Microcontroller main function flowchart

The main function source file also contains the UART receiving interrupt, where the command system is implemented. The command system receives and decodes commands from the computer client in packages of 8 bits. For normal commands, such as gain setting, the computer client needs to send the command header first to tell the microcontroller that the following data are commands for different channels. Then the computer client can send over commands in a format of "channel number + gain value". Both channel number and gain value are in 8-bit formats. The computer client can send the same format multiple times for different channels, until the setting finish command is sent. There are also two special commands that do not need the command header. They are "Go" and "Stop" commands that control the start and stop operation of the sampling process. Even though the command system is implemented, most

of it is not used currently implemented in the program due to the fact that the compatible graphical user interface is not developed.

8.2 Computer

On the computer side, the project team developed a program with MATLAB to control the project device. Figure 66 shows operation details of the MATLAB script through a flowchart. The MATLAB script communicates with the microcontroller through a serial port. The serial port setting matches the UART setting in the microcontroller: 128000 baud rate, one stop bit, and no parity. The main processing loop of the script is also a three-state machine. The first state asks for user input to determine the desired number of samples. There are five options: 1, 250, 500, 750, and 1000. The script sends the corresponding command to the microcontroller to set the number of samples. In the second state, the script asks for user input to start the sample process. Then MATLAB pulls data from the serial buffer in packages of 8 bits. These data are rebuilt into regular 24-bit data and converted into voltage values. In the third state, all flags and variables are reset to prepare for the next cycle. Users can choose to start the sampling process all over again if it is necessary.

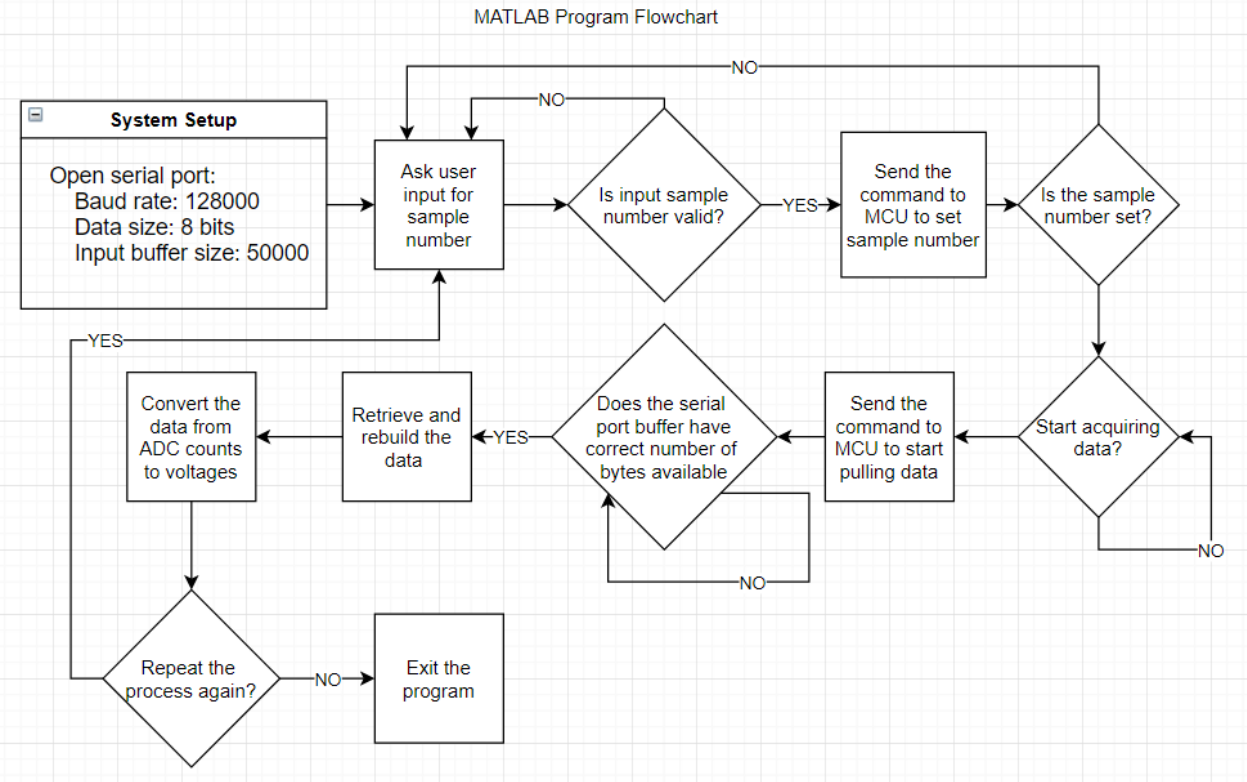

Figure 66: MATLAB Script Flowchart

9 Performance

This section details the performance of each area of our EMG acquisition device.

9.1 Electrode Assembly

One major consideration of the electrode assembly was the introduction of noise into the circuit as the noise past this first stage will be divided by the gains of each following stage. The noise of the instrumentation amplifier was required to be ideally under 1 uVrms when referred to input. These tests included connecting the electrode amplifier's inputs and passing the resulting output signal through an operational amplifier with a specific measured gain. In order to calculate the referred to input noise, the RMS reading from an oscilloscope was divided by the gain of each stage. These tests resulted in a RTI voltage noise of 0.693 uVrms, thus being below the required 1 uVrms. Note that this noise level is specified for between the frequencies of 13 Hz, from the high pass filter cutoff in the instrumentation amplifier, and 1200 Hz, from the gain bandwidth product of the instrumentation amplifier used in testing.

Additional requirements of the electrode amplifier were a gain of 50 V/V while still being able to be powered by the USB port on a computer. The cutoff frequency was also required to pass frequencies in the range of the signal of interest, between 20 Hz and 1000 Hz. With the current design, the output signal can be amplified close to the power supply rails of +/- 3.3 V, although any expected EMG signal multiplied by a gain of 50 V/V will never reach this limit. As shown in Figure 67, the maximum gain reaches roughly 34.5 dB in the measured values which corresponds to 53.5 V/V. Also note that the cutoff frequency is roughly 13 Hz, allowing the magnitude to reach close to the full magnitude at the start of the EMG frequency range. Figure

64 below also demonstrates the accuracy of the completed electrode assembly when compared to the ideal values. The fluctuation from ideal can be attributed to component tolerances.

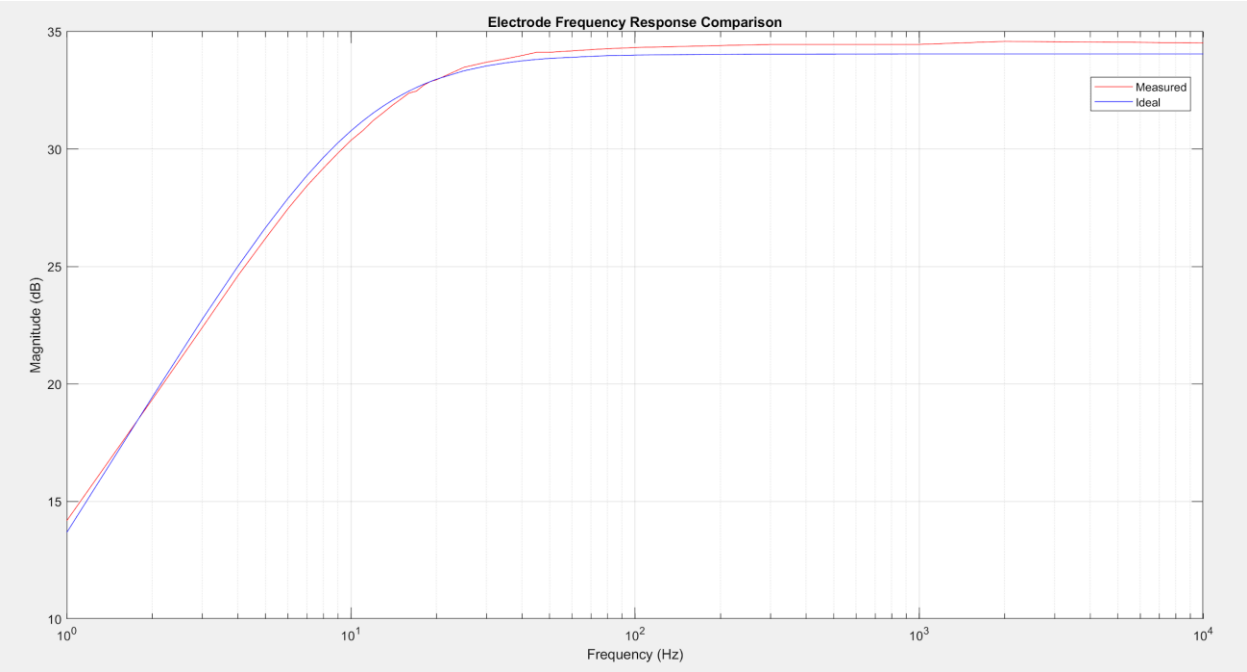

Figure 67: Electrode Frequency Response Comparison

An additional requirement of the electrode amplifier was to have a Common Mode Rejection Ratio of greater than 100 dB at 60 Hz. According to the datasheet for the chosen instrumentation amplifier (AD8220), the CMRR at 60 Hz should be roughly 120 dB at 50 V/V. With the equipment available to us, the team measured 103 dB at 70 Hz. Note that 70 Hz was chosen as to not have interference from the power line. It should also be noted that the size of the electrodes was required to be as small as possible to fit many around the arm of a subject.

As previously noted, the size was vastly reduced in this iteration of electrode amplifier design. The electrode amplifier developed throughout this project is slightly larger than the 2015 passive electrode assembly (measuring roughly 3.0 cm tall x 0.6 cm wide x 0.2 cm thick),

however, it includes electronics inside. One of the additional electrical components used in this design is a capacitor used to provide additional gain and high pass filter characteristics, leading to lower expected electronics noise. Another component that lead to size reduction was the introduction of modified PEM nuts as a way to mount the electrodes. With all the electrical components used in the current version of the electrode assembly, the size is vastly improved from previous active electrode designs, as noted in Table 3 below.

Table 3: Dimensions for Electrodes

Electrode Assembly	Height (cm)	Width (cm)	Thickness (cm)
2005 Active Electrode	3.8	1.6	1.1
Silicone Body Electrode	3.18	1.14	0.48
Resin Encasement	3.18	1.27	0.55
3D Printed Encasement with Resin Resin Fill (Our Design)	3.18	1.19	0.51

9.2 Signal Processing PCB

The signal processing PCB is powered primarily from a USB 2.0 female connector. The USB 2.0 connector will always be connected to the local PC during operation and receives a 5 V power supply up to 500 mA of current from the PC. Power provided from the PC is isolated using a power isolating chip, which can source up to 400 mA of current. This system eliminates both isolated and earth-grounded power supplies in comparison to the 2005 system. During sampling the supply current used is <300mA, which fits in our original design specifications and the capacity of the power isolation chip. Various voltages are required to correctly operate different chips on the PCB. The full list of used voltages are as follows: 2.5 V, -2.5 V, 3.3 V, -3.3 V, 5 V.

The signal coming from the electrode assembly would enter a filtering stage before it was digitized by our ADS1298 ADCs. This filtering stage consisted of a 2nd order Sallen-Key high pass filter followed by an RC low pass filter. The tested cutoff for the high pass filter was 15 Hz and the low pass cutoff was around 4 kHz. This stage had a base gain of 5, which in combination with our electrode channels produced the specified 250 V/V gain from the design specifications.

The ADS1298s are powered with 2.5 V and -2.5 V for analog rails, and 3.3 V for digital signals. Each channel has internal PGAs which have gain options of 1, 2, 3, 4, 6, 8, and 12 V/V and can be sampled up to 32 kHz. Figure 68 below shows the noise power spectrum when the signal processing PCB input channels are grounded, which was tested to be 0.034 uVrms RTI. With the measured electrode noise, the overall system noise was calculated to be 0.694 uVrss RTI.

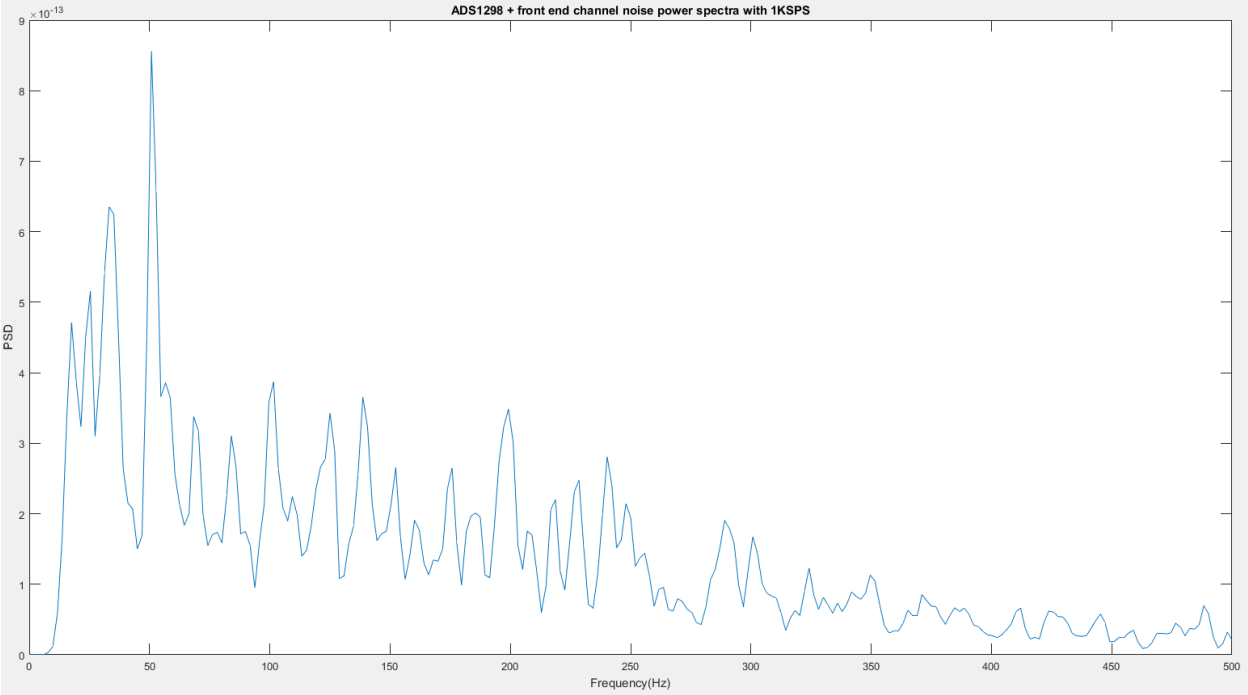

Figure 68: ADS1298 + Front End Channel Noise Power Spectra with 1 kSPS

From this figure, the highest concentration of noise is centered at around 60 Hz, which is commonly seen in power line interference. The ADS1298 uses a sinc^3 digital filter, which has a 3 dB cutoff frequency at about 0.262 multiplied by the sampling rate. Figure 69 shows the tested frequency response (in red) of ADS1298 versus the one given in the datasheet (in blue). It is obvious that the tested results generally agree with the frequency response given in the datasheet. Therefore, to avoid 3 dB cutoff in the signal bandwidth of interest, the sampling rate needs to be set to four times as large as the desired Nyquist frequency (or the low pass effect of the sinc filter otherwise counteracted). From the ADC functional testing, the test results indicated that ADS1298 has a measured DC offset of 0.0178 V at inputs.

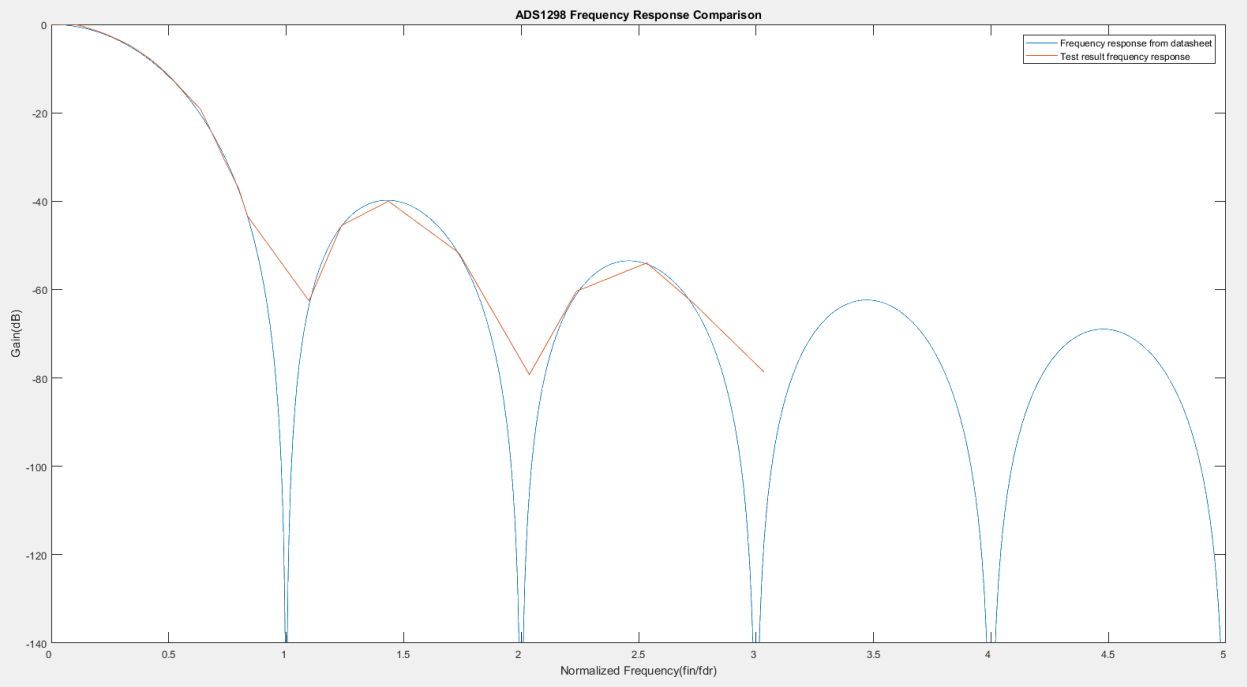

Figure 69: ADS1298 frequency response comparison

The ADS1298 transfers data to the microcontroller using an SPI interface. The microcontroller uses a system clock of 32 MHz and operated the SPI clock at 16 MHz. After software processing, data are sent over the UART to be converted into serial communication protocols using an FTDI UART to Serial conversion chip. Data are sent at 128,000 bps over the UART, which goes through a signal isolation chip before being received by the PC. However, the microcontroller used in the current device is not fast enough to pull data out of both ADCs at the desired data rate. Thus, only one ADC is functional at 1 kSPS in our prototype. Figure 70 shows the raw EMG signal measured from human biceps muscle contraction through the project device. The signal pattern matches the muscle contraction movements.

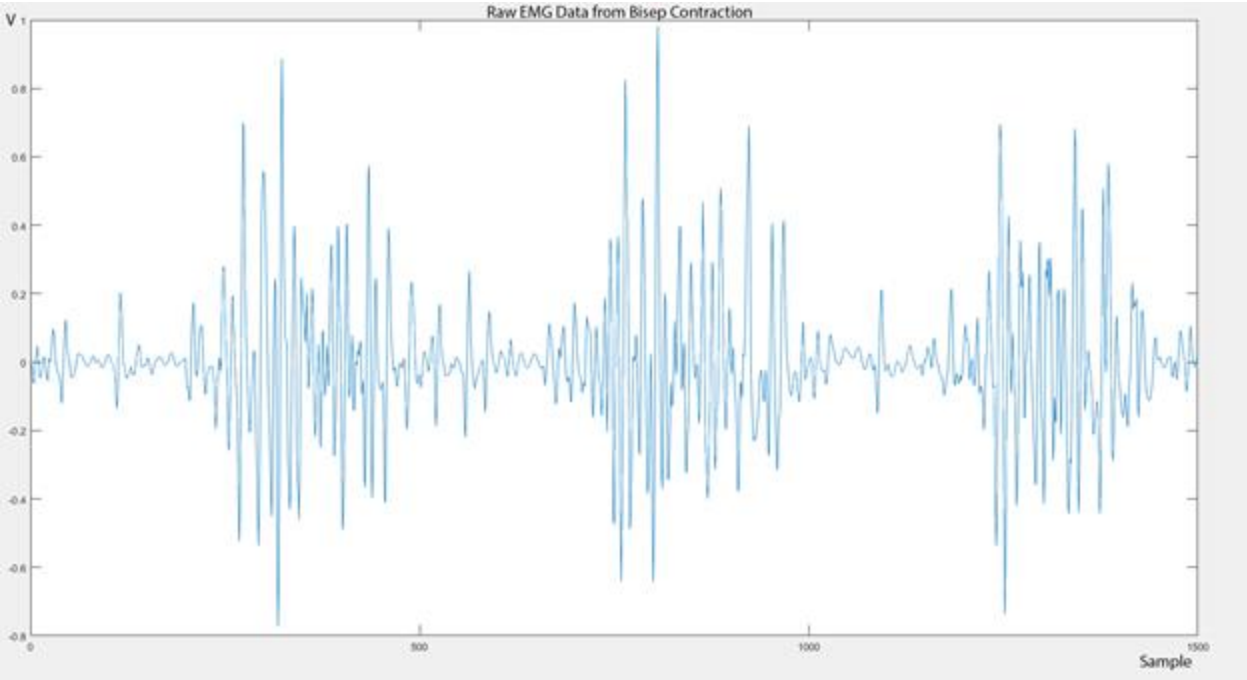

Figure 70: Raw EMG Signal Measured from Bicep Muscle Contraction

10 Discussion

The key accomplishments of the project are creating a system that can accept a signal input voltage range of 0.1 mV to 10 mV, with a large fixed gain of 250 V/V, a high input impedance of 10^4 GΩ, with selectable gain levels (1, 2, 3, 4, 6, 8, and 12 V/V) from the ADS1298s, 4.8 V of dynamic range on the 24-bit ADC, a digitally isolated system that no longer requires a medically isolated power supply, and a total current consumption of less than 300 mA. The current system also uses a smaller profile electrode amplifier while incorporating electronics inside. The current design is also much smaller than previous systems, measuring roughly 3” x 5” x 4”. The current system provides gains without having to use manual switches, as well as provides electrodes that are easy to replace and that use the abundant micro-USB connector.

Even though the electrode design from this project has similar dimensions as the ones from previous designs, the current electrode design is an active electrode, which means it contains electronics inside, while the 2015 design only acts as contact points. Nonetheless, there are still ways to reduce the size of the current electrode design with built in electronics. During the design process of the current electrode, the difficulty level of manufacturing the electrode in an academic environment was considered. Therefore, the electronic component size and packaging were selected so that the circuit board could be completed by hand-soldering. If the circuit board could be manufactured professionally and smaller packaging sizes could be used. Thus, the size of the electrode could be reduced. Welding the contacting bolts directly to the circuit board could also further reduce the size of the electrode, since a large copper contacting ring is not necessary anymore.

Due to limited time and resources, the final product of the project does not meet all of the design requirements specified in the early design stage, which leaves room for further

improvements. The project device cannot accommodate the full desired input bandwidth, 20-1000 Hz. The main cause of the performance degeneration is the limitation in microcontroller speed. The microcontroller needs to be fast enough to pull out sampling data from two ADS1298s when they are operating at various sampling rates. The higher the sampling rate, the faster the microprocessor needs to run. With the current microcontroller, the project device can only support one ADS1298 operation with up to 1000 samples per second (SPS) sampling rate. Figure 68 shows a segment of one thousand output samples with an input of 100 Hz, 3 V pk-pk sine wave at 1 kSPS. The plotted waveform is as expected according to the input signal. However, when the sampling rate is increased to 2 kSPS, the output data plot does not appear to be correct anymore. Figure 72 shows a segment of one thousand output samples at 2 kSPS with the same input signal. Notice that with the 100 Hz input signal and 2 kSPS, the number of periods of the sine wave should be half as many as are shown in Figure 72. It indicates that the ADC actually output two thousand samples within the sampling period, but the microcontroller skipped samples and only grabbed one thousand samples. The reason why the microcontroller skips samples is its operating speed limitation. The microcontroller is not fast enough to grab the sample data before the new data are available. The speed limitation was also proved by examining the SPI communication between the ADC and microcontroller using a digital analyzer.

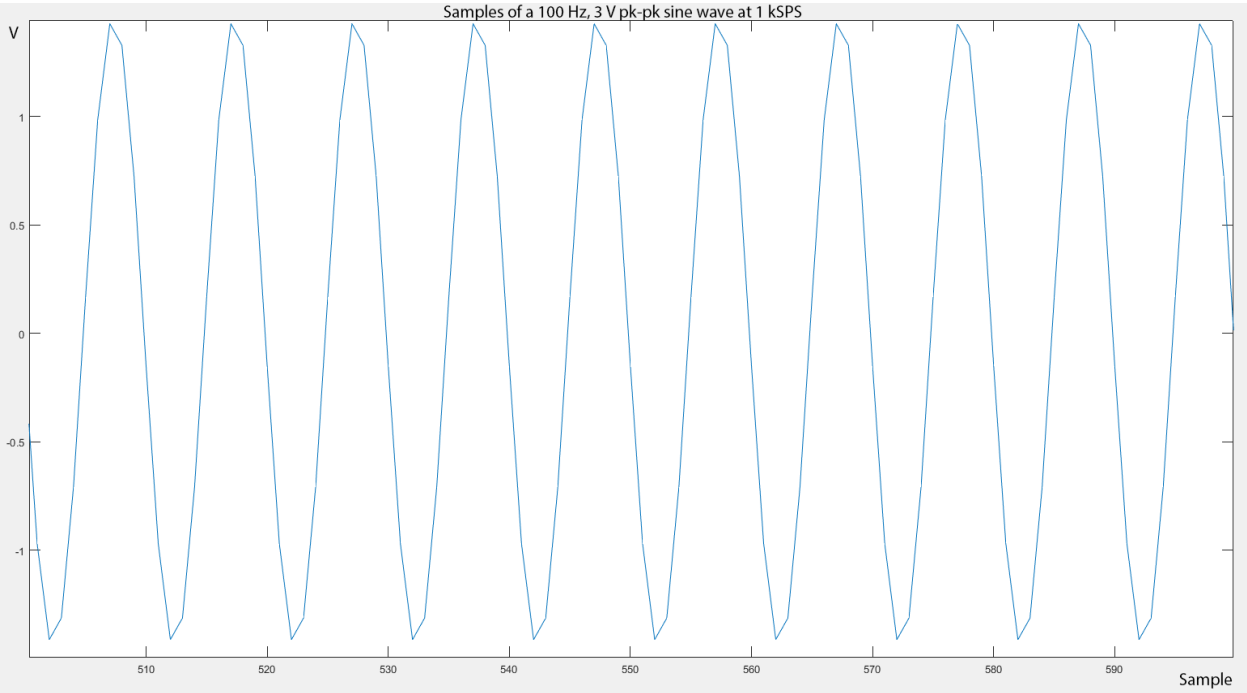

Figure 71: A segment of output data with an input of 100 Hz, 3 V pk-pk sine wave at 1 kSPS

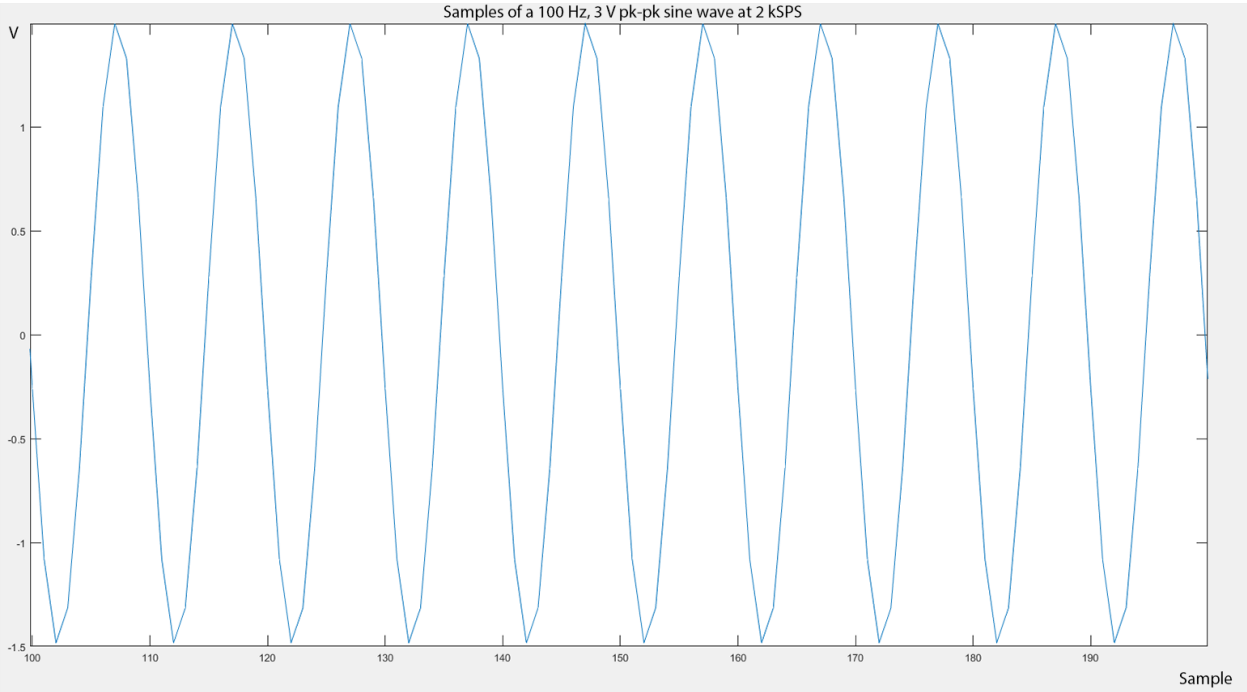

Figure 72: A segment of output data with an input of 100 Hz, 3 V pk-pk sine wave at 2 kSPS

The level of speed required to run smoothly at the highest possible sampling rate is unknown, however, the ADS1298ECG-FE evaluation kit from Texas Instruments which uses the same ADC has a Digital Signal Processor (DSP) chip running at a clock rate of 200 MHz (compared to the 32 MHz rate used in this project design). As a result, the project team recommends using a fast DSP or FPGA chip in order to achieve higher clock frequencies. Since there are several ECE classes using FPGA boards, a FPGA chip may be easier to use with the resources available at WPI. Additionally, many of these boards can be found in evaluation platforms in order to make testing easier.

Due to the speed issue, the current microcontroller program does not support continuous sampling mode. Users are required to pre-select the desired number of samples before starting the sampling process. Then the program will produce the same number of samples as specified. If the speed issue can be resolved, the continuous sampling mode can be implemented to provide real time EMG data.

With a faster data processing unit, more functions can be integrated, such as selectable lower sample data output rate. Currently the sample data output rate is the same as the data rate of the operating ADCs. The ADS1298 provides data rates of 500 SPS, 1 kSPS, 2 kSPS, 4 kSPS, 8 kSPS, 16 kSPS, and 32 kSPS. Higher data rates allow wider input bandwidth. Some users may want higher input bandwidth but a lower sample data output rate. Thus, a digital low pass filter and a decimation function are necessary. A faster data processing unit can support these functions without encountering the speed issues.

The device performance is also limited by the limited ADC selections available on the market. ADS1298 is the only ADC on the market that meets our design requirements. However, it uses a $sinc^3$ digital filter which is shown in Figure 69. The $sinc^3$ digital filter has a 3dB cutoff

frequency that is 0.262 times the data rate. The cutoff frequency is only about half of the Nyquist frequency. A possible solution is to run the ADS1298 at a high data rate that provides a Nyquist frequency that is twice as large as the desired Nyquist frequency. However, running at a higher data rate would require the microcontroller to run even faster. If the microcontroller could not provide the required operating speed, a digital shaping filter could be implemented to counteract the 3 dB point rolloff to provide a wider pass band. Another possible solution is to look for an ADC that has a better digital filter. According to an application report from Texas Instruments, there are other types of digital filters used in Delta-Sigma ADCs, such as the wideband filter shown in Figure 73. The digital filter shown in Figure 73 has a cutoff frequency that is much closer to the Nyquist frequency compared to the $sinc^3$ filter. However, as mentioned before, the ADS1298 was the only ADC on the market when the device was developed that meet the design requirements.

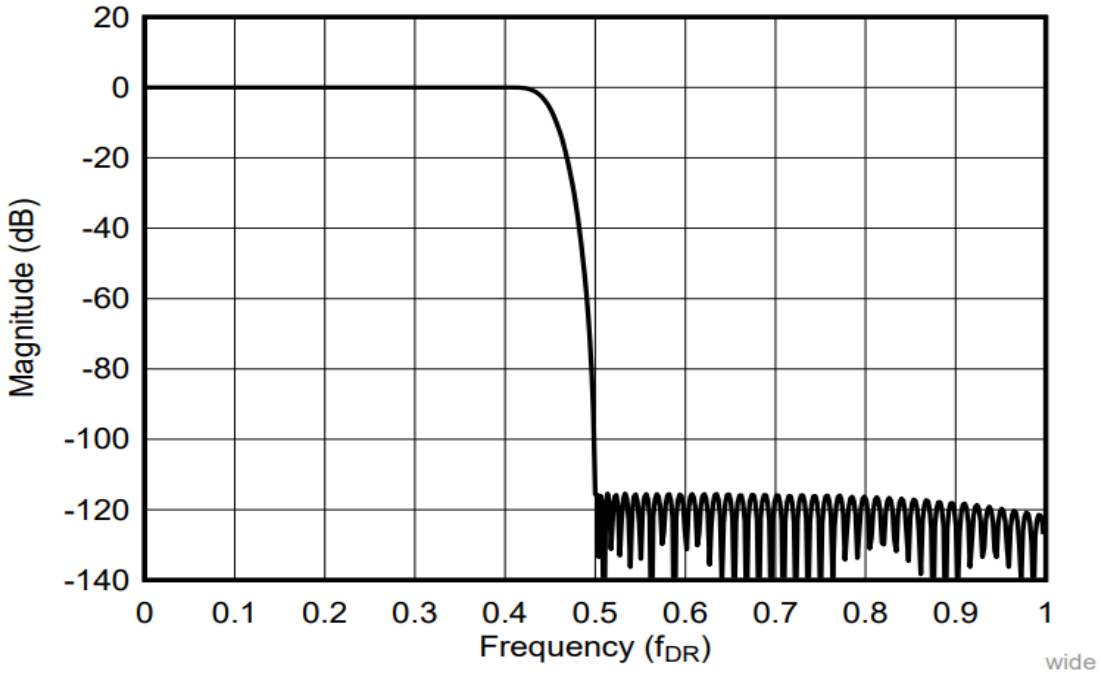

Figure 73: Wideband Filter Frequency Response (Pisani, 2017)

Another improvement for the device is implementing software gain. One of the reasons to use 24-bit ADCs is to take advantage of the excessive sampling resolution. The desired sampling resolution for this project device is 16 bits. By using 24-bit ADCs, the extra bits can be used to accommodate for instrumental noise and implement software gains. This space is seen as "headroom" so that the maximum possible input will never fully saturate the device and lose information about the voltage level of the input signal. The software gain can be implemented with simple bit manipulations on the ADC data, which can be done either on the microcontroller or MATLAB. If the software gain is implemented on the microcontroller, the microcontroller needs to be fast enough to accommodate the extra computation time required. It also needs additional codes to separate software gain values from the PGA gain values. If the software gain is implemented in MATLAB, the microcontroller needs to send 24-bit ADC data over the USB instead of 16-bit data. The MATLAB script will need to take care of the bit manipulations. By using the internal PGAs and software gains, more gain options can be made available to users.

As electronics becomes smaller and smaller and integrated circuits becomes more and more powerful, it is possible to have a more compact design in the future. We have considered the idea that integrated everything up until the microcontroller to the electrodes. This integration would mean that the instrumentation amplifier, front end analog channel, and a single channel 24-bit ADC would all be put on the electrode circuit board. It could be a most compact design if the sizes of the ADC and other components are small enough. However, the device would also be more difficult to design and manufacture. A new power solution would be necessary to deliver different voltages from the main board to the electrodes. It would be more difficult to find available components on the market that fit both size and performance requirements. In order to make the electrode board space efficient, the design needs to use small component

packages, which are not meant to be soldered by hand. The software design would also be more challenging, since the signal processor unit needs to communicate with multiple ADCs at the same time. If the above difficulties could be resolved, a more advanced and compact design would not be far away.

11 Conclusion

Our project team went through the research and design process and developed a compact EMG acquisition system based on our design requirements. The electrode amplifier was improved from the previous version, integrating the instrumentation amplifier circuit into the main encasement of the electrode case while keeping a smaller profile than the original, while the inclusion of a cutoff capacitor and gain resistor allowed for higher gain. The encasement method and materials were also improved for easier production. The use of PEM nuts and steel bolts also helped reduce the overall electrode assembly profile while keeping a good conductive contact between the electrode and the electrode PCB.

The use of the ADS1298 on the signal processing PCB allowed the entire EMG system to be medically isolated by using on-board power and signal isolation chips, reducing electrical power requirements. Previous iterations used PCIe ADCs, which were not able to be isolated unless the entire computer was isolated. The ADS1298s also had individual PGAs for each channel, eliminating the use of external gain setting chips. Since the ADC was of the sigma delta family, each input provided a high sampling rate, which made the low pass anti-aliasing filters easier to implement.

The finished EMG device also made large improvements in power consumption. With the use of low power microcontrollers, ADCs, and OP-amps, the entire system could be easily powered by the 500mA 5V power supply given by any PC USB 2.0 port. By removing the isolated power supply brick used in previous designs, the current prototype is by far the smallest and most portable version available.

With everything that our project team has accomplished, it is still possible to further improve our EMG acquisition system.

References

Ahamed, Nizam Uddin, et al. "Age-Related EMG Responses of the Biceps Brachii Muscle of Young Adults." *Biomedical Research* (2016). 787-789. Web.

Argie, Roxanne, and Alvin Burt. *Synaptic Transmission*., Biology: Q-Z (2016). 146-149. Print.

Burke, David. "Whither Needle EMG?" *Clinical Neurophysiology* 121.9 (2010): 1373-5. Print.

Clancy, Edward. *Design of a High-Resolution, Monopolar, Surface Electromyogram (EMG) Array Electrode-Amplifier and its Associated Signal Conditioning Circuit*., 2002. 7-21. Report.

---. *EMG-Force Acquisition System*., 2015. 1-11. Report.

"DT9826 Series." *Measurement Computing.* Web. December 18, 2017.

Sheingold, Daniel H.. *Analog-to-Digital Converter*. McGraw-Hill Education, 2014. Web.

Lee, Herrington. "EMG Biofeedback: What can it Actually Show." *Physiotherapy* 82.10 (1996): 581-3. Web.

Lerner, K. L. "Action Potential." *The Gale Encyclopedia of Science.* Eds. K. Lee Lerner and Brenda Wilmoth Lerner. 5th ed. ed. Farmington Hills, MI: Gale, 2014. Web.

Merletti, Roberto, Dario Farina, Wiley-Blackwell Online Books. *Surface Electromyography: Physiology, Engineering and Applications*. Hoboken, New Jersey; Piscataway, NJ: IEEE Press, 2016. 33-75, 333-356. Print.

Pisani, Brian. *Digital Filter Types in Delta-Sigma ADCs*. Texas Instruments, 2017, *Digital Filter Types in Delta-Sigma ADCs*. 3. Web.

Ravariu, Cristian. "Contributions to Novel Methods in Electrophysiology Aided by Electronic Devices and Circuits." *Applied Biomedical Engineering.* Eds. Gaetano D. Gargiulo and Alistair McEwan. Rijeka: InTech, 2011. Ch. 06. Print.

Slater, Clarke R. "The Functional Organization of Motor Nerve Terminals." *Progress in neurobiology* 134 (2015): 55-103. *MEDLINE database.* Web.

Thornton, Rachel, and Andrew Michell. "Techniques and Applications of EMG: Measuring Motor Units from Structure to Function." *Journal of Neurology* 259.3 (2012): 585-94. *MEDLINE database.* Web.

Webster, John G., and John W. Clark. *Medical Instrumentation: Application and Design*. 4th ed. Hoboken, NJ: John Wiley & Sons, 2010. 145, 198-210, 666. Print.

Appendix A: PCB Bill of Materials

CATEGORY	PACKAGE	NAME	PCB DESIGNATORS	QTY/UNIT	MANUFACTURER	P/N (DIGI)
MAIN BOARD	Metric/Imperial					
Resistors						
1% Tolerance	1005/402	466K	R5, R6, R17, R18, R29, R30, R41, R42, R53, R54, R65, R66, R77, R78, R89, R90	16	Yageo	YAG3167CT-ND
		82.3K	R7, R10, R19, R22, R31, R34, R43, R46, R55, R58, R67, R70, R79, R82, R91, R94	16	Yageo	311-82.5KLRCT-ND
		400	R8, R11, R20, R23, R32, R35, R44, R47, R56, R59, R68, R71, R80, R83, R92, R95	16	Yageo	YAG3152CT-ND
		142K	R9, R13, R21, R25, R33, R37, R45, R49, R57, R61, R69, R73, R81, R85, R93, R97	16	Yageo	YAG2979CT-ND
		100K	R12, R14, R24, R26, R36, R38, R48, R50, R60, R62,	16	Yageo	311-100KLRCT-ND

			R72, R74, R84, R86, R96, R98			
		20.6K	R15, R16, R27, R28, R39, R40, R51, R52, R63, R64, R75, R76, R87, R88, R99, R100	16	Yageo	YAG3052CT-ND
	1608/603	10K	R1, R2, R3, R4, R118	5	Yageo	311-10.0KHRCT-ND
		NI	R101, R102	2	Yageo	N/A
		50K	R106	1	Yageo	311-49.9KHRCT-ND
		46.4K	R107	1	Yageo	311-46.4KHRCT-ND
		47.5K	R108	1	Yageo	311-47.5KHRCT-ND
		43.2K	R109	1	Yageo	311-43.2KHRCT-ND
		63.9K	R110	1	Yageo	311-63.4KHRCT-ND

		35.9K	R111	1	Yageo	311-36.0KHRCT-ND
		4.7K	R112	1	Yageo	311-4.70KHRCT-ND
		1K	R113	1	Yageo	311-1.00KHRCT-ND
		325	R114, R115	2	Yageo	311-324HRCT-ND
		470	R117, R119	2	Yageo	311-470HRCT-ND
		24	R120, R121, R122, R123	4	Yageo	311-24.0HRCT-ND
Capacitors						
10% Tolerance	1005/402	62nF	C40, C41, C42, C43, C46, C47, C48, C49, C58, C59, C60, C61, C70, C71, C72, C73, C76, C77, C78, C79, C82, C83, C84, C85, C88, C89, C90, C91, C94, C95, C96, C97	32	Murata Elec	490-12709-1-ND
		100nF	C44, C45, C56, C57, C68, C69, C74, C75, C80, C81,	16	Murata Elec	490-6328-1-ND

			C86, C87, C92, C93, C98, C99			
		1uF	C50, C52, C54, C66	4	Samsung	1276-1067-1-ND
		0.1uF	C51, C53, C55, C67	4	Murata Elec	490-6328-1-ND
	1608/603	1uF	C1, C3, C7, C8, C11, C13, C15, C16, C18, C20, C22, C26, C27, C28, C32, C34, C35, C37, C39, C101, C104, C106, C109, C113, C114, C118, C123, C128, C130, C132	30	KEMET	399-3118-1-ND
		470pF	C107	1	Murata Elec	490-1367-1-ND
		2.2uF	C108, C111, C116, C119, C121, C124, C126	7	Murata Elec	490-3296-1-ND
		22uF	C14, C33	2	Murata Elec	490-7611-1-ND
		0.1uF	C2, C4, C10, C12, C17, C19, C21, C23, C29, C31, C36, C38, C129, C131, C133, C135, C137, C138, C139, C140, C141	21	KEMET	399-1095-1-ND
		10uF	C9, C30, C100, C102, C103, C105, C110, C112, C115, C117, C120, C122, C125, C127, C134, C136	16	Samsung	1276-1038-1-ND

Inductors						
	1608/603	470Ohm @ 100MHz	L1, L2, L6, L7, L8, L9	6	TDK	445-5218-1-ND
		120Ohm @ 100MHz	L3, L10	2	Taiyo Yuden	587-1923-1-ND
		ACM7060	L4, L5	2	TDK	445-2215-1-ND
Connectors						
	Male	Header 3	J1	1	Samtec	SAM1035-03-ND
	Female	USB A	J2	1	Molex	WM4078-ND
	Female	Barrel Jack	J3	1	CUI	CP-040DH-ND
	Female	Header 6	J4	1	Amphenol FCI	609-3263-ND
	Female	Header 6X2A	J5	1	Sullins	S7074-ND
	Female	Header 4X2A	J6, J10	2	Sullins	S5674-ND
	Female	Header 2	J7, J8, J9, J11, J12, J13	6	Sullins	S5633-ND
LEDs		LED2	LED4, LED5	2	Lite-On	160-1456-1-ND
Test Points		Test Point	TP1, TP3, TP8, TP11, TP14, TP18, TP19, TP20, TP21, TP22, TP23, TP24,	18	Keystone	36-5002-ND

			TP25, TP26, TP27, TP28, TP29, TP30			
ICs		ADS1298_PAG_64	U1, U2	2	Texas Instruments	296-27734-ND
		ADC CLK	U3	1	ECS	XC1635CT-ND
		OPA4170	U4, U5, U14, U15	4	Texas Instruments	296-29664-1-ND
		ADUM4160BRWZ	U6	1	Analog Devices	ADUM4160BRWZ-RLTR-ND
		Power Isolator	U24	1	Recom	945-1764-5-ND
		TPS60403DBVR	U25	1	Texas Instruments	296-27005-1-ND
		TPS73233	U26	1	Texas Instruments	296-39483-1-ND
		TPS73201	U27	1	Texas Instruments	296-32554-1-ND
		TPS72301	U28, U29	2	Texas Instruments	296-27049-1-ND
		PIC24FJ128GA204-I_PT	U30	1	Microchip	PIC24FJ128GA204-I/PT-ND
		FT232RL	U31	1	FTDI	768-1007-1-ND
		Push Button	U32, U33, U34	3	TE Connectivity	450-1650-ND

PERIPHERAL BOARD						
	Female	MICRO USB B	U1 - 8	8	CUI	102-4006-1-ND
	Male	SMD Header 4x2	J1	1	Molex	WM17458-ND
	Male	SMD Header 2x1	J2 - 4	3	Samtec	SAM8979-ND
ELECTRODE ASSEMBLY						
		AD8220		1	Analog Devices	AD8220ARMZ-R7CT-ND
	805	16uF		1	Taiyo Yuden	587-1300-1-ND
	805	1K		1	Yageo	311-1.00KHRCT-ND
	805	0.1uF		2	KEMET	399-1095-1-ND
ACCESSORIES						

		2P Shunt		1	Samtec	SAM8858-ND
	M3	12mm Spacer (male-female)		2	McMaster	
	M3	12 mm spacer (female to female)		2	McMaster	
		18mm spacer (female-female)		4	McMaster	